

Variational inference for approximate objective priors using neural networks

Nils Baillie¹ Université Paris-Saclay, CEA, Service d'Études Mécaniques et Thermiques, 91191 Gif-sur-Yvette, France

CMAP, CNRS, École polytechnique, Institut Polytechnique de Paris, 91120 Palaiseau, France
Antoine Van Biesbroeck Université Paris-Saclay, CEA, Service d'Études Mécaniques et Thermiques, 91191 Gif-sur-Yvette, France

CMAP, CNRS, École polytechnique, Institut Polytechnique de Paris, 91120 Palaiseau, France
Clément Gauchy Université Paris-Saclay, CEA, Service de Génie Logiciel pour la Simulation, 91191 Gif-sur-Yvette, France

Date published: 2025-08-26 Last modified: 2025-08-26

Abstract

In Bayesian statistics, the choice of the prior can have an important influence on the posterior and the parameter estimation, especially when few data samples are available. To limit the added subjectivity from a priori information, one can use the framework of objective priors, more particularly, we focus on reference priors in this work. However, computing such priors is a difficult task in general. Hence, we consider cases where the reference prior simplifies to the Jeffreys prior. We develop in this paper a flexible algorithm based on variational inference which computes approximations of priors from a set of parametric distributions using neural networks. We also show that our algorithm can retrieve modified Jeffreys priors when constraints are specified in the optimization problem to ensure the solution is proper. We propose a simple method to recover a relevant approximation of the parametric posterior distribution using Markov Chain Monte Carlo (MCMC) methods even if the density function of the parametric prior is not known in general. Numerical experiments on several statistical models of increasing complexity are presented. We show the usefulness of this approach by recovering the target distribution. The performance of the algorithm is evaluated on both prior and posterior distributions, jointly using variational inference and MCMC sampling.

Keywords: Reference priors, Variational inference, Neural networks

1 Contents

2	1 Introduction	2
3	2 Reference priors theory	4
4	3 Variational approximation of the reference prior (VA-RP)	7
5	3.1 Implicitly defined parametric probability distributions using neural networks	7
6	3.2 Learning the VA-RP using stochastic gradient algorithm	8
7	3.3 Adaptation for the constrained VA-RP	10
8	3.4 Posterior sampling using implicitly defined prior distributions	12

¹Corresponding author: nils.baillie@cea.fr

9	4 Numerical experiments	13
10	4.1 Multinomial model	14
11	4.2 Probit model	18
12	5 Conclusion	24
13	Acknowledgement	24
14	6 Appendix	25
15	6.1 Gradient computation of the generalized mutual information	25
16	6.2 Gaussian distribution with variance parameter	26
17	6.3 Probit model and robustness	28
18	References	32

19 **1 Introduction**

20 The Bayesian approach to statistical inference aims to produce estimations using the posterior
 21 distribution. The latter is derived by updating the prior distribution with the observed statistics
 22 thanks to Bayes' theorem. However, the shape of the posterior can be heavily influenced by the
 23 prior choice when the amount of available data is limited or when the prior distribution is highly
 24 informative. For this reason, selecting a prior remains a daunting task that must be handled carefully.
 25 Hence, systematic methods have been introduced by statisticians to help in the choice of the prior
 26 distribution, both in cases where subjective knowledge is available or not (Press (2009)). Kass and
 27 Wasserman (1996) propose different ways of defining the level of non-informativeness of a prior
 28 distribution. The most famous method is the Maximum Entropy (ME) prior distribution that has
 29 been popularized by Jaynes (1957). In a Bayesian context, ME and Maximal Data Information (MDI)
 30 priors have been studied by Zellner (1996), Soofi (2000). Other candidates for objective priors are the
 31 so-called matching priors (Reid, Mukerjee, and Fraser (2003)), which are priors such that the Bayesian
 32 posterior credible intervals correspond to confidence intervals of the sampling model. Moreover,
 33 when a simpler model is known, the Penalizing Complexity (PC) priors are yet another rationale of
 34 choosing an objective (or reference) prior distribution (Simpson et al. (2017)).

35 In this paper, we will focus on the reference prior theory. First introduced in Bernardo (1979a) and
 36 further formalized in Berger, Bernardo, and Sun (2009), the main rationale behind the reference
 37 prior theory is the maximization of the information brought by the data during Bayesian inference.
 38 Specifically, reference priors (RPs) are constructed to maximize the mutual information metric, which
 39 is defined as a divergence between itself and the posterior. In this way, it ensures that the data plays
 40 a dominant role in the Bayesian framework. There is consensus that the definition of RPs in high
 41 dimensions should be more subtle than simply maximizing the mutual information (see e.g. Berger,
 42 Bernardo, and Sun (2015)). A common approach consists in a hierarchical construction of reference
 43 priors, firstly mentioned in Bernardo (1979b) and detailed further in Berger and Bernardo (1992b). In
 44 this approach, an ordering is imposed on groups of parameters, and the reference prior is derived by
 45 sequentially maximizing the mutual information for each group.

46 Reference priors are used in various statistical models, such as Gaussian process-based models
 47 (Paulo (2005), Gu and Berger (2016)), generalized linear models (Natarajan and Kass (2000)), and even
 48 Bayesian Neural Networks (Gao, Ramesh, and Chaudhari (2022)). The RPs are recognized for their
 49 objective nature in practical studies (D'Andrea (2021), Li and Gu (2021), Van Biesbroeck et al. (2024)),
 50 yet they suffer from their low computational feasibility. Indeed, the expression of the RPs often leads
 51 to an intricate theoretical expression, which necessitates a heavy numerical cost to be derived that

52 becomes even more cumbersome as the dimensionality of the problem increases. Moreover, in many
53 applications, a posteriori estimates are obtained using Markov Chain Monte Carlo (MCMC) methods,
54 which require a large number of prior evaluations, further compounding the computational burden.
55 The hierarchical construction of reference priors aggravates this problem even more, for that reason,
56 we will focus solely on the maximization of the mutual information, which corresponds to the special
57 case where no ordering is imposed on the parameters. In this context, it has been shown by Clarke
58 and Barron (1994), and more recently by Van Biesbroeck (2024a) in a more general case, that the
59 Jeffreys prior (Jeffreys (1946)) is the prior that maximizes the mutual information when the number
60 of data samples tends to infinity. Hence, it will serve as the target distribution in our applications.

61 In general, when we look for sampling or approximating a probability distribution, several approaches
62 arise and may be used within a Bayesian framework. In this work, we focus on variational infer-
63 ence methods. Variational inference seeks to approximate a complex target distribution p , —e.g. a
64 posterior— by optimizing over a family of simpler parameterized distributions q_λ . The goal then is
65 to find the distribution q_{λ^*} that is the best approximation of p by minimizing a divergence, such as
66 the Kullback-Leibler (KL) divergence. Variational inference methods have been widely adopted in
67 various contexts, including popular models such as Variational Autoencoders (VAEs) (Kingma and
68 Welling (2019)), which are a class of generative models where one wants to learn the underlying
69 distribution of data samples. We can also mention normalizing flows (Papamakarios et al. (2021),
70 Kobyzev, Prince, and Brubaker (2021)), which consider diffeomorphism transformations to recover
71 the density of the approximated distribution from the simpler one taken as input.

72 Variational inference seems especially relevant in a context where one wants to approximate prior
73 distributions defined as maximizers of a given metric. This kind of approach was introduced in
74 Nalisnick and Smyth (2017) and Gauchy et al. (2023) in order to approximate the Jeffreys prior in
75 one-dimensional models. The main difference being the choice of the objective function. In Nalisnick
76 and Smyth (2017), the authors propose a variational inference procedure using a lower bound of the
77 mutual information as an optimization criterion, whereas in Gauchy et al. (2023), stochastic gradient
78 ascent is directly applied on the mutual information criterion.

79 By building on these foundations, this paper proposes a novel variational inference algorithm designed
80 to approximate reference priors by maximizing mutual information. Specifically, we focus on the
81 case where no ordering is imposed on the parameters, in which case the reference prior coincides
82 with the Jeffreys prior. For simplicity, we refer to them as variational approximations of the reference
83 priors (VA-RPs).

84 As in Nalisnick and Smyth (2017) and Gauchy et al. (2023), the Jeffreys prior is approximated in a
85 parametric family of probability distributions implicitly defined by the push-forward probability
86 distribution through a nonlinear function (see e.g. Papamakarios et al. (2021) and Marzouk et al.
87 (2016)). We will focus in this paper to push-forward probability measures through neural networks.
88 In comparison with the previous works, we benchmark extensively our algorithm on statistical
89 models of different complexity and nature to assess its robustness. We also extend our algorithm
90 to handle a more general case where a generalized mutual information criterion is defined using
91 f -divergences (Van Biesbroeck (2024a)). In this paper, we restrict the different benchmarks to α -
92 divergences. Additionally, we extend the framework to allow the integration of linear constraints
93 on the prior in the pipeline. That last feature permits handling situations where the Jeffreys prior
94 may be improper (i.e. it integrates to infinity). Improper priors pose a challenge because (i) one can
95 not sample from the a priori distribution, and (ii) they do not ensure that the posterior is proper,
96 jeopardizing a posteriori inference. Recent work detailed in Van Biesbroeck (2024b) introduces
97 linear constraints that ensure the proper aspects of priors maximizing the mutual information. Our
98 algorithm incorporates these constraints, providing a principled way to address improper priors and
99 ensuring that the resulting posterior distributions are well-defined and suitable for practical use.

100 First, we will introduce the reference prior theory of Bernardo (1979b) and the recent developments
 101 around generalized reference priors made by Van Biesbroeck (2024a) in Section 2. Next, the methodol-
 102 ogy to construct VA-RPs is detailed in Section 3. A stochastic gradient algorithm is proposed, as well
 103 as an augmented Lagrangian algorithm for the constrained optimization problem, for learning the
 104 parameters of an implicitly defined probability density function that will approximate the target prior.
 105 Moreover, a mindful trick to sample from the posterior distribution by MCMC using the implicitly
 106 defined prior distribution is proposed. In Section 4, different numerical experiments from various
 107 test cases are carried out in order to benchmark the VA-RP. Analytical statistical models where the
 108 Jeffreys prior is known are tested to allow comparison between the VA-RP and the Jeffreys prior.

109 2 Reference priors theory

110 The reference prior theory fits into the usual framework of statistical inference. The situation is the
 111 following: we observe i.i.d data samples $\mathbf{X} = (X_1, \dots, X_N) \in \mathcal{X}^N$ with $\mathcal{X} \subset \mathbb{R}^d$. We suppose that the
 112 likelihood function $L_N(\mathbf{X} | \theta) = \prod_{i=1}^N L(X_i | \theta)$ is known and $\theta \in \Theta \subset \mathbb{R}^q$ is the parameter we want to
 113 infer. Since we use the Bayesian framework, θ is considered to be a random variable with a prior
 114 distribution π . We also define the marginal likelihood $p_{\pi, N}(\mathbf{X}) = \int_{\Theta} \pi(\theta) L_N(\mathbf{X} | \theta) d\theta$ associated to the
 115 marginal probability measure $\mathbb{P}_{\pi, N}$. The non-asymptotic RP, first introduced in Bernardo (1979a) and
 116 formalized in Berger, Bernardo, and Sun (2009), is defined to be one of the priors verifying:

$$117 \pi^* \in \operatorname{argmax}_{\pi \in \mathcal{P}} I(\pi; L_N), \quad (1)$$

118 where \mathcal{P} is a class of admissible probability distributions and $I(\pi; L_N)$ is the mutual information for
 119 the prior π and the likelihood L_N between the random variable of the parameters $\theta \sim \pi$ and the
 random variable of the data $\mathbf{X} \sim \mathbb{P}_{\pi, N}$:

$$120 I(\pi; L_N) = \int_{\mathcal{X}^N} \text{KL}(\pi(\cdot | \mathbf{X}) \| \pi) p_{\pi, N}(\mathbf{X}) d\mathbf{X} \quad (2)$$

121 Hence, π^* is a prior that maximizes the Kullback-Leibler divergence between itself and its posterior
 122 averaged by the marginal distribution of datasets. The Kullback-Leibler divergence between two
 probability measures of density p and q defined on a generic set Ω writes:

$$123 \text{KL}(p \| q) = \int_{\Omega} \log\left(\frac{p(\omega)}{q(\omega)}\right) p(\omega) d\omega.$$

124 Thus, π^* is the prior that maximizes the influence of the data on the posterior distribution, justifying
 125 its reference (or objective) properties. The prior π^* can also be interpreted using channel coding
 126 and information theory (MacKay (2003), chapter 9). Indeed, remark that $I(\pi; L_N)$ corresponds to the
 127 mutual information $I(\theta, \mathbf{X})$ between the random variable $\theta \sim \pi$ and the data $\mathbf{X} \sim \mathbb{P}_{\pi, N}$, it measures
 128 the information that conveys the data \mathbf{X} about the parameters θ . The maximal value of this mutual
 129 information is defined as the channel's capacity. π^* thus corresponds to the prior distribution that
 maximizes the information about θ conveyed by the data \mathbf{X} .

130 Using Fubini's theorem and Bayes' theorem, we can derive an alternative and more practical expres-
 131 sion for the mutual information:

$$132 I(\pi; L_N) = \int_{\Theta} \text{KL}(L_N(\cdot | \theta) \| p_{\pi, N}) \pi(\theta) d\theta. \quad (3)$$

133 A more generalized definition of mutual information has been proposed in Van Biesbroeck (2024a)
 using f -divergences. The f -divergence mutual information is defined by

$$134 I_{D_f}(\pi; L_N) = \int_{\Theta} D_f(p_{\pi, N} \| L_N(\cdot | \theta)) \pi(\theta) d\theta, \quad (4)$$

134 with

$$D_f(p\|q) = \int_{\Omega} f\left(\frac{p(\omega)}{q(\omega)}\right) q(\omega) d\omega,$$

135 where f is usually chosen to be a convex function mapping 1 to 0. Remark that the classical mutual
136 information is obtained by choosing $f = -\log$, indeed, $D_{-\log}(p\|q) = \text{KL}(q\|p)$. The formal RP is
137 defined as N goes to infinity, but in practice we are restricted to the case where N takes a finite value.
138 However, the limit case $N \rightarrow +\infty$ is relevant because it has been shown in Clarke and Barron (1994),
139 Van Biesbroeck (2024a) that the solution of this asymptotic problem is the Jeffreys prior when the
140 mutual information is expressed as in Equation 2, or when it is defined using an α -divergence, as in
141 Equation 4 with $f = f_\alpha$, where:

$$f_\alpha(x) = \frac{x^\alpha - \alpha x - (1 - \alpha)}{\alpha(\alpha - 1)}, \quad \alpha \in (0, 1). \quad (5)$$

142 The Jeffreys prior, denoted by J , is defined as follows:

$$J(\theta) \propto \det(\mathcal{J}(\theta))^{1/2} \quad \text{with} \quad \mathcal{J}(\theta) = - \int_{\mathcal{X}^N} \frac{\partial^2 \log L_N}{\partial \theta^2}(\mathbf{X}|\theta) \cdot L_N(\mathbf{X}|\theta) d\mathbf{X}.$$

143 We suppose that the likelihood function is smooth such that the Fisher information matrix \mathcal{J} is well-
144 defined. The Jeffreys prior and the RP have the relevant property to be “invariant by reparametriza-
145 tion”:

$$\forall \varphi \text{ diffeomorphism}, \quad J(\theta) = \left| \frac{\partial \varphi}{\partial \theta} \right| \cdot J(\varphi(\theta)).$$

146 This property expresses non-information in the sense that if there is no information on θ , there
147 should not be more information on $\varphi(\theta)$ when φ is a diffeomorphism: an invertible and differentiable
148 transformation.

149 Actually, the historical definition of RPs involves the KL-divergence in the definition of the mutual
150 information. Yet the use of α -divergences instead is relevant because they can be seen as a continuous
151 path between the KL-divergence and the Reverse-KL-divergence when α varies from 0 to 1. We can
152 also mention that for $\alpha = 1/2$, the α -divergence is the squared Hellinger distance whose square root
153 is a metric since it is symmetric and verifies the triangle inequality.

154 Technically, the formal RP is constructed such that its projection on every compact subset (or open
155 subset in Muré (2018)) of Θ maximizes asymptotically the mutual information, which allows for
156 improper distributions to be RPs in some cases. The Jeffreys prior is itself often improper.

157 In our algorithm we consider probability distributions defined on the space Θ and not on sequences
158 of subsets. A consequence of this statement is that our algorithm may tend to approximate improper
159 priors in some cases. Indeed, any given sample by our algorithm results, by construction, from a
160 proper distribution, which is expected to be a good approximation of the solution of the optimization
161 problem expressed in Equation 1. This approach is justified to some extent since in the context of
162 Q-vague convergence defined in Bioche and Druilhet (2016) for instance, improper priors can be
163 the limit of sequences of proper priors. Although this theoretical notion of convergence is defined,
164 no concrete metric is given, making quantification of the difference between proper and improper
165 priors infeasible in practice.

166 The term “reference prior” is now associated with a more general, hierarchical construction. We
167 mentioned in the introduction the hierarchical construction of the reference prior, we present rapidly
168 the case where the dimension $q = 2$, i.e. $\theta = (\theta_1, \theta_2) \in \Theta_1 \times \Theta_2$ with θ_1 and θ_2 being in their own
169 separate groups:

170 • We obtain the first level conditional prior: $\pi_1^*(\cdot | \theta_2)$ on θ_1 by maximizing asymptotically the
 171 mutual information with fixed θ_2 in the likelihood L_N .
 172 • We define the second level likelihood using the previous prior as follows:

$$L'_N(X | \theta_2) = \int_{\Theta_1} L_N(X | \theta_1, \theta_2) \pi_1^*(\theta_1 | \theta_2) d\theta_1.$$

173 • We define and solve the corresponding asymptotic optimization problem with this function as
 174 our main likelihood function so we can obtain the second level prior: π_2^* on θ_2 .
 175 • This defines the hierarchical RP on θ , which is of the form: $\pi^*(\theta) = \pi_1^*(\theta_1 | \theta_2) \pi_2^*(\theta_2)$.

176 This construction can be extended to any number of groups of parameters with any ordering as
 177 presented in Berger and Bernardo (1992b). However, it is important to note that priors defined
 178 through this procedure can still be improper.

179 In summary, we introduced several priors: the Jeffreys prior, the non-asymptotic RP that maximizes
 180 the generalized mutual information, which depends on the chosen f -divergence and the value of
 181 N , the formal RP, that is obtained such that its projection on every (compact) subset maximizes
 182 asymptotically the generalized mutual information, hence it only depends on the f -divergence, and
 183 finally, the reference prior in the hierarchical sense. The latter reduces to the formal RP (i) in the
 184 one-dimensional case and (ii) in the multi-dimensional case, when all components of θ are placed
 185 in the same group. We will always be in one of these two cases in the following. In very specific
 186 situations, where the likelihood function is non-regular (Ghosal and Samanta (1997)) or because of
 187 the choice of f (Liu et al. (2014)), the formal RP and the Jeffreys prior can be different. However, as
 188 long as the likelihood is smooth which is verified for most statistical models and the KL-divergence
 189 or the α -divergence with $\alpha \in (0, 1)$ is used, these two priors are actually the same.

190 The algorithm we develop aims at solving the mutual information optimization problem with N
 191 fixed, thus our target prior is technically the non-asymptotic RP, nevertheless, the latter has no
 192 closed form expression, making the validation of the algorithm infeasible. If N is large enough, this
 193 prior should be close to the formal RP which is equal to the Jeffreys prior in this framework. Hence,
 194 the Jeffreys prior serves as the target prior in the numerical applications because it can either be
 195 computed explicitly or approximated through numerical integration.

196 Furthermore, as mentioned in the introduction, improper priors can also compromise the validity of
 197 a posteriori estimates in some cases. To address this issue, we adapted our algorithm to handle the
 198 developments made in Van Biesbroeck (2024b), which suggest a method to define proper objective
 199 priors by simply resolving a constrained version of the initial optimization problem:

$$\tilde{\pi}^* \in \underset{\substack{\pi \text{ prior} \\ \text{s.t. } \mathcal{C}(\pi) < \infty}}{\operatorname{argmax}} I_{D_{f_\alpha}}(\pi; L_N), \quad (6)$$

200 where $\mathcal{C}(\pi)$ defines a constraint of the form $\int_{\Theta} a(\theta) \pi(\theta) d\theta$, a being a positive function. When the
 201 mutual information in the above optimization problem is defined from an α -divergence, and when a
 202 verifies

$$\int_{\Theta} J(\theta) a(\theta)^{1/\alpha} d\theta < \infty \quad \text{and} \quad \int_{\Theta} J(\theta) a(\theta)^{1+1/\alpha} d\theta < \infty, \quad (7)$$

203 the author has proven that the constrained solution $\tilde{\pi}^*$ asymptotically takes the following form:

$$\tilde{\pi}^*(\theta) \propto J(\theta) a(\theta)^{1/\alpha},$$

204 which is proper. This result implies that in the case where constraints are imposed, the target prior
 205 becomes this modified version of the Jeffreys prior.

206 3 Variational approximation of the reference prior (VA-RP)

207 3.1 Implicitly defined parametric probability distributions using neural networks

208 Variational inference refers to techniques that aim to approximate a probability distribution by solving
209 an optimization problem —that often takes a variational form, such as maximizing evidence lower
210 bound (ELBO) (Kingma and Welling (2014)). It is thus relevant to consider them for approximating
211 RPs, as the goal is to maximize, w.r.t. the prior, the mutual information defined in Equation 3.

212 We restrict the set of priors to a parametric space $\{\pi_\lambda, \lambda \in \Lambda\}$, $\Lambda \subset \mathbb{R}^L$, reducing the original
213 optimization problem into a finite-dimensional one. The optimization problem in Equation 1 or
214 Equation 6 becomes finding $\underset{\lambda \in \Lambda}{\operatorname{argmax}} I_{D_f}(\pi_\lambda; L_N)$. Our approach is to define the set of priors π_λ
215 implicitly, as in Gauchy et al. (2023):

$$\theta \sim \pi_\lambda \iff \theta = g(\lambda, \varepsilon) \quad \text{and} \quad \varepsilon \sim \mathbb{P}_\varepsilon.$$

216 Here, g is a measurable function parameterized by λ , typically a neural network with λ corresponding
217 to its weights and biases, and we impose that g is differentiable with respect to λ . The variable ε can
218 be seen as a latent variable. It has an easy-to-sample distribution \mathbb{P}_ε with a simple density function.
219 In practice we use the centered multivariate Gaussian $\mathcal{N}(0, \mathbb{I}_{p \times p})$. The construction described above
220 allows the consideration of a vast family of priors. However, except in very simple cases, the density
221 of π_λ is not known and cannot be evaluated. Only samples of $\theta \sim \pi_\lambda$ can be obtained.

222 In the work of Nalisnick and Smyth (2017), this implicit sampling method is compared to several
223 other algorithms used to learn RPs in the case of one-dimensional models, where the RP is always the
224 Jeffreys prior. Among these methods, we can mention an algorithm proposed by Berger, Bernardo,
225 and Sun (2009) which does not sample from the RP but only evaluates it for specific points, or an
226 MCMC-based approach by Lafferty and Wasserman (2001), which is inspired from the previous one
227 but can sample from the RP.

228 According to this comparison, implicit sampling is, in the worst case, competitive with the other
229 methods, but achieves state-of-the-art results in the best case. Hence, computing the variational
230 approximation of the RP, which we will refer to as the VA-RP, seems to be a promising technique. We
231 admit that the term VA-RP is a slight abuse of terminology in our case since (i) the target prior is the
232 (eventually constrained) Jeffreys prior, which is not necessarily the reference prior when an ordering
233 is imposed on the parameters; and (ii) there is no guarantee that this target prior can be actually
234 reproduced by the neural network. Indeed, the VA-RP tends to be the prior that maximizes the
235 mutual information for a fixed value of N , within a family of priors that is, by design, parameterized
236 by λ . Since we are aware of those approximations, we strive to assess that our priors are good
237 approximations of the target priors in our numerical experiments.

238 The situations presented by Gauchy et al. (2023) and Nalisnick and Smyth (2017) are in dimension
239 one and use the Kullback-Leibler divergence within the definition of the mutual information.

240 The construction of the algorithm that we propose in the following accommodates multi-dimensional
241 modeling. It is also compatible with the extended form of the mutual information, as defined in
242 Equation 3 from an f -divergence.

243 The choice of the neural network is up to the user, we will showcase in our numerical applications
244 mostly simple networks, composed of one fully connected linear layer and one activation function.
245 However, the method can be used with deeper networks, such as normalizing flows (Papamakarios
246 et al. (2021)), or larger networks obtained through a mixture model of smaller networks utilizing the
247 “Gumbel-Softmax trick” (Jang, Gu, and Poole (2017)) for example. Such choices lead to more flexible
248 parametric distributions, but increase the difficulty of fine-tuning hyperparameters.

249 3.2 Learning the VA-RP using stochastic gradient algorithm

250 The VA-RP is formulated as the solution to the following optimization problem:

$$\pi_{\lambda^*} = \operatorname{argmax}_{\lambda \in \Lambda} \mathcal{O}_{D_f}(\pi_{\lambda}; L_N), \quad (8)$$

251 where π_{λ} is parameterized through the relation between a latent variable ε and the parameter θ , as
252 outlined in the preceding Section. The function \mathcal{O}_{D_f} is called the objective function, it is maximized
253 using stochastic gradient optimization, following the approach described in Gauchy et al. (2023).

254 It is intuitive to fix \mathcal{O}_{D_f} to equal I_{D_f} in order to maximize the mutual information of interest. In this
255 Section, we suggest alternative objective functions that can be considered to compute the VA-RP.
256 Our method is adaptable to any objective function \mathcal{O}_{D_f} that satisfies the following definition.

257 **Definition 1.** An objective function $\mathcal{O}_{D_f} : \lambda \in \Lambda \mapsto \mathcal{O}_{D_f}(\pi_{\lambda}; L_N) \in \mathbb{R}$ is said to be admissible if there
258 exists a mapping $\tilde{\mathcal{O}}_{D_f} : \Theta \rightarrow \mathbb{R}$ such that the gradient of \mathcal{O}_{D_f} w.r.t. $\lambda = (\lambda_1, \dots, \lambda_L)$ is

$$\frac{\partial \mathcal{O}_{D_f}}{\partial \lambda_l}(\pi_{\lambda}; L_N) = \mathbb{E}_{\varepsilon} \left[\sum_{j=1}^q \frac{\partial \tilde{\mathcal{O}}_{D_f}}{\partial \theta_j}(g(\lambda, \varepsilon)) \frac{\partial g_j}{\partial \lambda_l}(\lambda, \varepsilon) \right] \quad (9)$$

259 for any $l \in \{1, \dots, L\}$.

260 Here, $\tilde{\mathcal{O}}_{D_f}$ is a generic notation for a function that depends in practice on f and the likelihood
261 function. We also assume that its gradient is computed using Monte Carlo sampling. The framework
262 of admissible objective functions allows for flexible implementation, as it permits the separation of
263 sampling and differentiation operations:

264

- 265 The gradient of $\tilde{\mathcal{O}}_{D_f}$ mostly relies on random sampling and depends only on the likelihood L_N and the function f .
- 266 The gradient of g is computed independently. In practice, it is possible to leverage usual differentiation techniques for the neural network. In our work, we rely on PyTorch’s automatic differentiation feature “autograd” (Paszke et al. (2019)).

267 This separation is advantageous as automatic differentiation tools—such as autograd—are well-suited
268 to differentiating complex networks but struggle with functions incorporating randomness.

269 This way, the optimization problem can be addressed using stochastic gradient optimization, approximating at each step the gradient in Equation 9 via Monte Carlo estimates. In our experiments,
270 the implementation of the algorithm is done with the popular Adam optimizer (Kingma and Ba
271 (2017)), with its default hyperparameters, $\beta_1 = 0.9$ and $\beta_2 = 0.999$. The learning rate is tuned more
272 specifically for each numerical benchmark.

273 Concerning the choice of objective function, we verify that in appendix Section 6.1

$$\begin{aligned} \frac{\partial I_{D_f}}{\partial \lambda_l}(\pi_{\lambda}; L_N) &= \mathbb{E}_{\varepsilon} \left[\sum_{j=1}^q F_j \cdot \frac{\partial g_j}{\partial \lambda_l}(\lambda, \varepsilon) \right] \\ &+ \mathbb{E}_{\theta \sim \pi_{\lambda}} \left[\mathbb{E}_{\mathbf{X} \sim L_N(\cdot | \theta)} \left[\frac{1}{L_N(\mathbf{X} | \theta)} \frac{\partial p_{\lambda}}{\partial \lambda_l}(\mathbf{X}) f' \left(\frac{p_{\lambda}(\mathbf{X})}{L_N(\mathbf{X} | \theta)} \right) \right] \right], \end{aligned} \quad (10)$$

274 where:

$$F_j = \mathbb{E}_{\mathbf{X} \sim L_N(\cdot | \theta)} \left[\frac{\partial \log L_N}{\partial \theta_j}(\mathbf{X} | \theta) F \left(\frac{p_{\lambda}(\mathbf{X})}{L_N(\mathbf{X} | \theta)} \right) \right],$$

275 with $F(x) = f(x) - x f'(x)$ and p_{λ} is a shortcut notation for $p_{\pi_{\lambda}, N}$ being the marginal distribution
276 under π_{λ} .

280 Remark that only the case $f = -\log$ is considered by Gauchy et al. (2023), but it leads to a sim-
 281 plification of the gradient since the second term vanishes. Each term in the above equations is
 282 approximated as follows:

$$\begin{cases} p_\lambda(\mathbf{X}) = \mathbb{E}_{\theta \sim \pi_\lambda}[L_N(\mathbf{X} | \theta)] \approx \frac{1}{T} \sum_{t=1}^T L_N(\mathbf{X} | g(\lambda, \varepsilon_t)) \quad \text{where } \varepsilon_1, \dots, \varepsilon_T \sim \mathbb{P}_\varepsilon \\ F_j \approx \frac{1}{U} \sum_{u=1}^U \frac{\partial \log L_N}{\partial \theta_j}(\mathbf{X}^u | \theta) F\left(\frac{p_\lambda(\mathbf{X}^u)}{L_N(\mathbf{X}^u | \theta)}\right) \quad \text{where } \mathbf{X}^1, \dots, \mathbf{X}^U \sim \mathbb{P}_{\mathbf{X} | \theta}. \end{cases} \quad (11)$$

283 In their work, Nalisnick and Smyth (2017) propose an alternative objective function to optimize, that
 284 we call B_{D_f} .

285 This function corresponds to a lower bound of the mutual information. It is derived from an upper
 286 bound on the marginal distribution and relies on maximizing the likelihood. Their approach is only
 287 presented for $f = -\log$, we generalize the lower bound for any decreasing function f :

$$B_{D_f}(\pi; L_N) = \int_{\Theta} \int_{\mathcal{X}^N} f\left(\frac{L_N(\mathbf{X} | \hat{\theta}_{MLE})}{L_N(\mathbf{X} | \theta)}\right) \pi(\theta) L_N(\mathbf{X} | \theta) d\mathbf{X} d\theta,$$

288 where $\hat{\theta}_{MLE}$ being the maximum likelihood estimator (MLE). It only depends on the likelihood and
 289 not on λ which simplifies the gradient computation:

$$\frac{\partial B_{D_f}}{\partial \lambda_l}(\pi_\lambda; L_N) = \mathbb{E}_\varepsilon \left[\sum_{j=1}^q \frac{\partial \tilde{B}_{D_f}}{\partial \theta_j}(g(\lambda, \varepsilon)) \frac{\partial g_j}{\partial \lambda_l}(\lambda, \varepsilon) \right],$$

290 where:

$$\frac{\partial \tilde{B}_{D_f}}{\partial \theta_j}(\theta) = \mathbb{E}_{\mathbf{X} \sim L_N(\cdot | \theta)} \left[\frac{\partial \log L_N}{\partial \theta_j}(\mathbf{X} | \theta) F\left(\frac{L_N(\mathbf{X} | \hat{\theta}_{MLE})}{L_N(\mathbf{X} | \theta)}\right) \right].$$

291 Its form corresponds to the one of an admissible objective function (Equation 9), with:

$$\tilde{B}_{D_f}(\theta) = \int_{\mathcal{X}^N} L_N(\mathbf{X} | \theta) f\left(\frac{L_N(\mathbf{X} | \hat{\theta}_{MLE})}{L_N(\mathbf{X} | \theta)}\right) d\mathbf{X}.$$

292 Given that $p_\lambda(\mathbf{X}) \leq \max_{\theta' \in \Theta} L_N(\mathbf{X} | \theta') = L_N(\mathbf{X} | \hat{\theta}_{MLE})$ for all λ , we have $B_{D_f}(\pi_\lambda; L_N) \leq I_{D_f}(\pi_\lambda; L_N)$.

293 Since f_α , used in α -divergence (Equation 5), is not decreasing, we replace it with \hat{f}_α defined hereafter,
 294 because $D_{f_\alpha} = D_{\hat{f}_\alpha}$:

$$\hat{f}_\alpha(x) = \frac{x^\alpha - 1}{\alpha(\alpha - 1)} = f_\alpha(x) + \frac{1}{\alpha - 1}(x - 1).$$

295 The use of this function results in a more stable computation overall. Moreover, one argument for
 296 the use of α -divergences rather than the KL-divergence, is that we have an universal and explicit
 297 upper bound on the mutual information:

$$I_{D_{f_\alpha}}(\pi; L_N) = I_{D_{\hat{f}_\alpha}}(\pi; L_N) \leq \hat{f}_\alpha(0) = \frac{1}{\alpha(1 - \alpha)}.$$

298 This bound can be an indicator on how well the mutual information is optimized, although there is
 299 no guarantee that it can be attained in general.

300 The gradient of the objective function B_{D_f} can be approximated via Monte Carlo, in the same manner
 301 as in Equation 11.

302 It requires to compute the MLE, which can also be done using samples of ε :

$$L_N(\mathbf{X} | \hat{\theta}_{MLE}) \approx \max_{t \in \{1, \dots, T\}} L_N(\mathbf{X} | g(\lambda, \varepsilon_t)) \quad \text{where} \quad \varepsilon_1, \dots, \varepsilon_T \sim \mathbb{P}_\varepsilon.$$

303 **3.3 Adaptation for the constrained VA-RP**

304 Reference priors and Jeffreys priors are often criticized, because they can lead to improper posteriors.
 305 However, the variational optimization problem defined in Equation 8 can be adapted to incorporate
 306 simple constraints on the prior. As mentioned in Section 2, there exist specific constraints that would
 307 make the theoretical solution proper.

308 This is also a way to incorporate expert knowledge to some extent. We consider K constraints of the
 309 form:

$$\forall k \in \{1, \dots, K\}, \quad \mathcal{C}_k(\pi_\lambda) = \mathbb{E}_{\theta \sim \pi_\lambda} [a_k(\theta)] - b_k,$$

310 with $a_k: \Theta \mapsto \mathbb{R}^+$ integrable and linearly independent functions, and $b_k \in \mathbb{R}$. We then adapt the
 311 optimization problem in Equation 8 to propose the following constrained optimization problem:

$$\begin{aligned} \pi_{\lambda^*}^C &\in \underset{\lambda \in \Lambda}{\operatorname{argmax}} \mathcal{O}_{D_f}(\pi_\lambda; L_N) \\ \text{subject to} \quad \forall k &\in \{1, \dots, K\}, \quad \mathcal{C}_k(\pi_\lambda) = 0, \end{aligned}$$

312 where $\pi_{\lambda^*}^C$ is the constrained VA-RP. The optimization problem with the mutual information has an
 313 explicit asymptotic solution for proper priors verifying the previous conditions:

314 • In the case of the KL-divergence (Bernardo (2005)):

$$\pi^C(\theta) \propto J(\theta) \exp \left(1 + \sum_{k=1}^K \nu_k a_k(\theta) \right).$$

315 • In the case of α -divergences (Van Biesbroeck (2024b)):

$$\pi^C(\theta) \propto J(\theta) \left(1 + \sum_{k=1}^K \nu_k a_k(\theta) \right)^{1/\alpha}.$$

316 where $\nu_1, \dots, \nu_K \in \mathbb{R}$ are constants determined by the constraints.

317 Recent work by Van Biesbroeck (2024b) makes it possible to build a proper objective prior under a
 318 relevant constraint function with α -divergence. The theorem considers $a: \Theta \mapsto \mathbb{R}^+$ which verifies
 319 the conditions expressed in Equation 7. Letting \mathcal{P}_a be the set of proper priors π on Θ such that
 320 $\pi \cdot a \in L^1$, the prior $\tilde{\pi}^*$ that maximizes the mutual information under the constraint $\tilde{\pi}^* \in \mathcal{P}_a$ is:

$$\tilde{\pi}^*(\theta) \propto J(\theta) a(\theta)^{1/\alpha}.$$

321 We propose the following general method to approximate the VA-RP under such constraints:

322 • Compute the VA-RP $\pi_\lambda \approx J$, in the same manner as for the unconstrained case.

323 • Estimate the constants \mathcal{K} and c using Monte Carlo samples from the VA-RP, as:

$$\mathcal{K}_\lambda = \int_{\Theta} \pi_\lambda(\theta) a(\theta)^{1/\alpha} d\theta \approx \int_{\Theta} J(\theta) a(\theta)^{1/\alpha} d\theta = \mathcal{K},$$

$$c_\lambda = \int_{\Theta} \pi_\lambda(\theta) a(\theta)^{1+(1/\alpha)} d\theta \approx \int_{\Theta} J(\theta) a(\theta)^{1+(1/\alpha)} d\theta = c.$$

325 • Since we have the equality:

$$\mathbb{E}_{\theta \sim \tilde{\pi}^*}[a(\theta)] = \int_{\Theta} \tilde{\pi}^*(\theta) a(\theta) d\theta = \frac{1}{\mathcal{K}} \int_{\Theta} J(\theta) a(\theta)^{1+(1/\alpha)} d\theta = \frac{c}{\mathcal{K}},$$

326 we compute the constrained VA-RP using the constraint: $\mathbb{E}_{\theta \sim \pi_{\lambda'}}[a(\theta)] = c_\lambda / \mathcal{K}_\lambda$ to approximate
327 $\pi_{\lambda'} \approx \tilde{\pi}^*$.

328 One might use different variational approximations for π_λ and $\pi_{\lambda'}$ because J and $\tilde{\pi}^*$ could have very
329 different forms depending on the function a .

330 The idea is to solve the constrained optimization problem as an unconstrained problem but with a
331 Lagrangian as the objective function. We take the work of Nocedal and Wright (2006) as support.

332 We denote η the Lagrange multiplier. Instead of using the usual Lagrangian function, Nocedal and
333 Wright (2006) suggest adding a term defined with $\tilde{\eta}$, a vector with positive components which serve
334 as penalization coefficients, and η' which can be thought of a prior estimate of η , although not in a
335 Bayesian sense. The objective is to find a saddle point (λ^*, η^*) which is a solution of the updated
336 optimization problem:

$$\max_{\lambda} \left(\min_{\eta} \mathcal{O}_{D_f}(\pi_\lambda; L_N) + \sum_{k=1}^K \eta_k \mathcal{C}_k(\pi_\lambda) + \sum_{k=1}^K \frac{1}{2\tilde{\eta}_k} (\eta_k - \eta'_k)^2 \right).$$

337 One can see that the third term serves as a penalization for large deviations from η' . The minimization
338 on η is feasible because it is a convex quadratic, and we get $\eta = \eta' - \tilde{\eta} \cdot \mathcal{C}(\pi_\lambda)$. Replacing η by its
339 expression leads to the resolution of the problem:

$$\max_{\lambda} \mathcal{O}_{D_f}(\pi_\lambda; L_N) + \sum_{k=1}^K \eta'_k \mathcal{C}_k(\pi_\lambda) - \sum_{k=1}^K \frac{\tilde{\eta}_k}{2} \mathcal{C}_k(\pi_\lambda)^2.$$

340 This motivates the definition of the augmented Lagrangian:

$$\mathcal{L}_A(\lambda, \eta, \tilde{\eta}) = \mathcal{O}_{D_f}(\pi_\lambda; L_N) + \sum_{k=1}^K \eta_k \mathcal{C}_k(\pi_\lambda) - \sum_{k=1}^K \frac{\tilde{\eta}_k}{2} \mathcal{C}_k(\pi_\lambda)^2.$$

341 Its gradient has a form that is compatible with our algorithm, as depicted in Section 3.2 (see Equa-
342 tion 9):

$$\begin{aligned} \frac{\partial \mathcal{L}_A}{\partial \lambda}(\lambda, \eta, \tilde{\eta}) &= \frac{\partial \mathcal{O}_{D_f}}{\partial \lambda}(\pi_\lambda; L_N) + \mathbb{E}_\varepsilon \left[\left(\sum_{k=1}^K \frac{\partial a_k}{\partial \theta}(g(\lambda, \varepsilon)) (\eta_k - \tilde{\eta}_k \mathcal{C}_k(\pi_\lambda)) \right) \frac{\partial g}{\partial \lambda}(\lambda, \varepsilon) \right] \\ &= \mathbb{E}_\varepsilon \left[\left(\frac{\partial \tilde{\mathcal{O}}}{\partial \theta}(g(\lambda, \varepsilon)) + \sum_{k=1}^K \frac{\partial a_k}{\partial \theta}(g(\lambda, \varepsilon)) (\eta_k - \tilde{\eta}_k \mathcal{C}_k(\pi_\lambda)) \right) \frac{\partial g}{\partial \lambda}(\lambda, \varepsilon) \right]. \end{aligned}$$

343 In practice, the augmented Lagrangian algorithm is of the form:

$$\begin{cases} \lambda^{t+1} = \underset{\lambda}{\operatorname{argmax}} \mathcal{L}_A(\lambda, \eta^t, \tilde{\eta}) \\ \forall k \in \{1, \dots, K\}, \eta_k^{t+1} = \eta_k^t - \tilde{\eta}_k \cdot \mathcal{C}_k(\pi_{\lambda^{t+1}}). \end{cases}$$

344 In our implementation, η is updated every 100 epochs. The penalty parameter $\tilde{\eta}$ can be interpreted
 345 as the learning rate of η , we use an adaptive scheme inspired by Basir and Senocak (2023) where
 346 we check if the largest constraint value $\|\mathcal{C}(\pi_\lambda)\|_\infty$ is higher than a specified threshold M or not. If
 347 $\|\mathcal{C}(\pi_\lambda)\|_\infty > M$, we multiply $\tilde{\eta}$ by v , otherwise we divide by v . We also impose a maximum value $\tilde{\eta}_{max}$.

348 3.4 Posterior sampling using implicitly defined prior distributions

349 Although our main object of study is the prior distribution, one needs to find the posterior distribution
 350 given an observed dataset \mathbf{X} in order to do the inference on θ . The posterior is of the form:

$$\pi_\lambda(\theta | \mathbf{X}) = \frac{\pi_\lambda(\theta) L_N(\mathbf{X} | \theta)}{p_\lambda(\mathbf{X})}.$$

351 As discussed in the introduction, one can approximate the posterior distribution when knowing
 352 the prior either by using MCMC or variational inference. In both cases, knowing the marginal
 353 distribution is not required. Indeed, MCMC samplers inspired by the Metropolis-Hastings algorithm
 354 can be applied, even if the posterior distribution is only known up to a multiplicative constant.
 355 The same can be said for variational approximation since the ELBO can be expressed without the
 356 marginal.

357 The issue here is that the density function $\pi_\lambda(\theta)$ is not explicit and can not be evaluated, except for
 358 very simple cases. However, we imposed that the distribution of the variable ε is simple enough, so
 359 one is able to evaluate its density. We propose to use ε as the variable of interest instead of θ because
 360 it lets us circumvent this issue. In practice, the idea is to reverse the order of operations: instead of
 361 sampling ε , then transforming ε into θ , which defines the prior on θ , and finally sampling posterior
 362 samples of θ given \mathbf{X} , one can proceed as follows:

363 • Define the posterior distribution on ε :

$$\pi_{\varepsilon, \lambda}(\varepsilon | \mathbf{X}) = \frac{p_\varepsilon(\varepsilon) L_N(\mathbf{X} | g(\lambda, \varepsilon))}{p_\lambda(\mathbf{X})},$$

364 where p_ε is the probability density function of ε . $\pi_{\varepsilon, \lambda}(\varepsilon | \mathbf{X})$ is known up to a multiplicative
 365 constant since the marginal p_λ is intractable in general. It is indeed a probability distribution
 366 on \mathbb{R}^p because:

$$p_\lambda(\mathbf{X}) = \int_{\Theta} \pi_\lambda(\theta) L_N(\mathbf{X} | \theta) d\theta = \int_{\mathbb{R}^p} L_N(\mathbf{X} | g(\lambda, \varepsilon)) dP_\varepsilon$$

367 • Sample posterior ε samples from the previous distribution, approximated by MCMC or varia-
 368 tional inference.

369 • Apply the transformation $\theta = g(\lambda, \varepsilon)$, and one gets posterior θ samples: $\theta \sim \pi_\lambda(\cdot | \mathbf{X})$.

370 More precisely, we denote for a fixed dataset \mathbf{X} :

$$\theta \sim \tilde{\pi}_\lambda(\cdot | \mathbf{X}) \iff \theta = g(\lambda, \varepsilon) \quad \text{with} \quad \varepsilon \sim \pi_{\varepsilon, \lambda}(\cdot | \mathbf{X}).$$

371 The previous approach is valid because $\pi_\lambda(\cdot | \mathbf{X})$ and $\tilde{\pi}_\lambda(\cdot | \mathbf{X})$ lead to the same distribution, as proven
 372 by the following derivation: let φ be a bounded and measurable function on Θ .

373 Using the definitions of the different distributions, we have that:

$$\begin{aligned}
\int_{\Theta} \varphi(\theta) \tilde{\pi}_{\lambda}(\theta | \mathbf{X}) d\theta &= \int_{\mathbb{R}^p} \varphi(g(\lambda, \varepsilon)) \pi_{\varepsilon, \lambda}(\varepsilon | \mathbf{X}) d\varepsilon \\
&= \int_{\mathbb{R}^p} \varphi(g(\lambda, \varepsilon)) \frac{p_{\varepsilon}(\varepsilon) L_N(X | g(\lambda, \varepsilon))}{p_{\lambda}(\mathbf{X})} d\varepsilon \\
&= \int_{\Theta} \varphi(\theta) \pi_{\lambda}(\theta) \frac{L_N(\mathbf{X} | \theta)}{p_{\lambda}(\mathbf{X})} d\theta \\
&= \int_{\Theta} \varphi(\theta) \pi_{\lambda}(\theta | \mathbf{X}) d\theta.
\end{aligned}$$

374 As mentioned in the last Section, when the Jeffreys prior is improper, we compare the posterior
375 distributions, namely, the exact reference posterior when available and the posterior obtained from
376 the VA-RP using the previous method. Altogether, we are able to sample θ from the posterior even if
377 the density of the parametric prior π_{λ} on θ is unavailable due to an implicit definition of the prior
378 distribution.

379 For our computations, we choose MCMC sampling, namely an adaptive Metropolis-Hastings sampler
380 with a multivariate Gaussian as the proposal distribution. The adaptation scheme is the following:
381 for each batch of iterations, we monitor the acceptance rate and we adapt the variance parameter of
382 the Gaussian proposal in order to have an acceptance rate close to 40%, which is the advised value
383 (Gelman et al. (2013)) for models in small dimensions. We refer to this algorithm as MH(ε). Because
384 we apply MCMC sampling on variable $\varepsilon \in \mathbb{R}^p$ with a reasonable value for p , we expect this step of
385 the algorithm to be fast compared to the computation of the VA-RP.

386 One could also use classic variational inference on ε instead, but the parametric set of distributions
387 must be chosen wisely. In VAEs for instance, multivariate Gaussian are often considered since it
388 simplifies the KL-divergence term in the ELBO. However, this might be too simplistic in our case
389 since we must apply the neural network g to recover θ samples. This means that the approximated
390 posterior on θ belongs to a very similar set of distributions to those used for the VA-RP, since we
391 already used a multivariate Gaussian for the prior on ε . On the other hand, applying once again
392 the implicit sampling approach does not exploit the additional information we have on $\pi_{\varepsilon, \lambda}(\varepsilon | \mathbf{X})$
393 compared to $\pi_{\lambda}(\theta)$, specifically, that its density function is known up to a multiplicative constant.
394 Hence, we argue that using a Metropolis-Hastings sampler is more straightforward in this situation.

395 4 Numerical experiments

396 We want to apply our algorithm to different statistical models, the first one is the multinomial model,
397 which is the simplest in the sense that the target distributions—the Jeffreys prior and posterior—
398 have explicit expressions and are part of a usual parametric family of proper distributions. The
399 second model—the probit model—will be highlighted with supplementary computations, in regards
400 to the assessment of the stability of our stochastic algorithm, and also with the addition of a moment
401 constraint.

402 The one-dimensional statistical model of the Gaussian distribution with variance parameter is also
403 presented in Section 6. We stress that this case is a toy model, where the target distributions, namely,
404 the Jeffreys prior and posterior, with or without constraints, can be derived exactly. Essentially, this
405 lets us verify that the output of the algorithm is relevant when compared to the true solution.

406 Since we only have to compute quotients of the likelihood or the gradient of the log-likelihood, we
407 can omit the multiplicative constant which does not depend on θ .

408 As for the output of the neural networks, the activation function just before the output is different
 409 for each statistical model, the same can be said for the learning rate. In some cases, we apply an
 410 affine transformation on the variable θ to avoid divisions by zero during training. In every test case,
 411 we consider simple networks for an easier fine-tuning of the hyperparameters and also because the
 412 precise computation of the loss function is an important bottleneck.

413 For the initialization of the neural networks, biases are set to zero and weights are randomly sampled
 414 from a Gaussian distribution. As for the several hyperparameters, we take $N = 10$, $T = 50$ and
 415 $U = 1000$ unless stated otherwise. We take a latent space of dimension $p = 50$. For the posterior
 416 calculations, we keep the last $5 \cdot 10^4$ samples from the Markov chain over a total of 10^5 Metropolis-
 417 Hastings iterations. Increasing N is advised in order to get closer to the asymptotic case for the
 418 optimization problem, and increasing U and T is relevant for the precision of the Monte Carlo estimates.
 419 Nevertheless, this increases computation times and we have to do a trade-off between the former
 420 and the latter. As for the constrained optimization, we use $v = 2$, $M = 0.005$ and $\tilde{\eta}_{max} = 10^4$.

421 4.1 Multinomial model

422 The multinomial distribution can be interpreted as the generalization of the binomial distribution
 423 for higher dimensions. We denote: $X_i \sim \text{Multinomial}(n, (\theta_1, \dots, \theta_q))$ with $n \in \mathbb{N}^*$, $\mathbf{X} \in \mathcal{X}^N$ and $\theta \in \Theta$,
 424 with: $\mathcal{X} = \{X \in \{0, \dots, n\}^q \mid \sum_{j=1}^q X^j = n\}$ and $\Theta = \{\theta \in (0, 1)^q \mid \sum_{j=1}^q \theta_j = 1\}$. We use $n = 10$ and
 425 $q = \dim(\theta) = 4$.

426 The likelihood function and the gradient of its logarithm are:

$$427 L_N(\mathbf{X} \mid \theta) = \prod_{i=1}^N \frac{n!}{X_i^1! \cdot \dots \cdot X_i^q!} \prod_{j=1}^q \theta_j^{X_i^j} \propto \prod_{i=1}^N \prod_{j=1}^q \theta_j^{X_i^j}$$

$$\forall (i, j), \frac{\partial \log L}{\partial \theta_j}(X_i \mid \theta) = \frac{X_i^j}{\theta_j}.$$

427 The MLE is available: $\forall j, \hat{\theta}_{MLE}(j) = \frac{1}{nN} \sum_{i=1}^N X_i^j$ and the Jeffreys prior is the $\text{Dir}_q\left(\frac{1}{2}, \dots, \frac{1}{2}\right)$ distribution,
 428 which is proper. The Jeffreys posterior is a conjugate Dirichlet distribution:

$$429 J_{post}(\theta \mid \mathbf{X}) = \text{Dir}_q(\theta; \gamma) \quad \text{with} \quad \gamma_j = \frac{1}{2} + \sum_{i=1}^N X_i^j.$$

429 We recall that the probability density function of a Dirichlet distribution of parameter γ is the
 430 following:

$$430 \text{Dir}_q(x; \gamma) = \frac{\Gamma(\sum_{j=1}^q \gamma_j)}{\prod_{j=1}^q \Gamma(\gamma_j)} \prod_{j=1}^q x_j^{\gamma_j - 1}.$$

431 We also use the fact that the marginal distributions of the Dirichlet distribution are Beta distributions,
 432 i.e., if $x \sim \text{Dir}_q(\gamma)$, then, for every $j \in \{1, \dots, q\}$, $x_j \sim \text{Beta}(\gamma_j, \sum_{k \neq j} \gamma_k)$. The Beta distribution can be
 433 seen as a particular case of Dirichlet distribution of dimension $q = 2$.

434 Although the Jeffreys prior is the prior that maximizes the mutual information, Berger and Bernardo
 435 (1992a) and Berger, Bernardo, and Sun (2015) argue that other priors for the multinomial model are
 436 more suited in terms of non-informativeness as the dimension of θ increases. According to them, an
 437 appropriate prior is the m -group reference prior, where the parameters are grouped into m groups on
 438 which a specific ordering is imposed ($1 \leq m \leq q$). The Jeffreys prior is the 1-group reference prior
 439 with this definition, while the authors suggest that the q -group one is more appropriate. Nevertheless,

440 our approach consists in approximating the prior yielding the highest mutual information when no
 441 ordering is imposed on the parameters, hence, the Jeffreys prior is still the target prior in this regard.
 442 We opt for a simple neural network with one linear layer and a Softmax activation function assuring
 443 that all components are positive and sum to 1. Explicitly, we have that:

$$\theta = \text{Softmax}(W\varepsilon + b),$$

444 with $W \in \mathbb{R}^{4 \times p}$ the weight matrix and $b \in \mathbb{R}^4$ the bias vector. The density function of θ does not
 445 have a closed expression. The following results are obtained with $\alpha = 0.5$ for the divergence and the
 446 lower bound is used as the objective function.

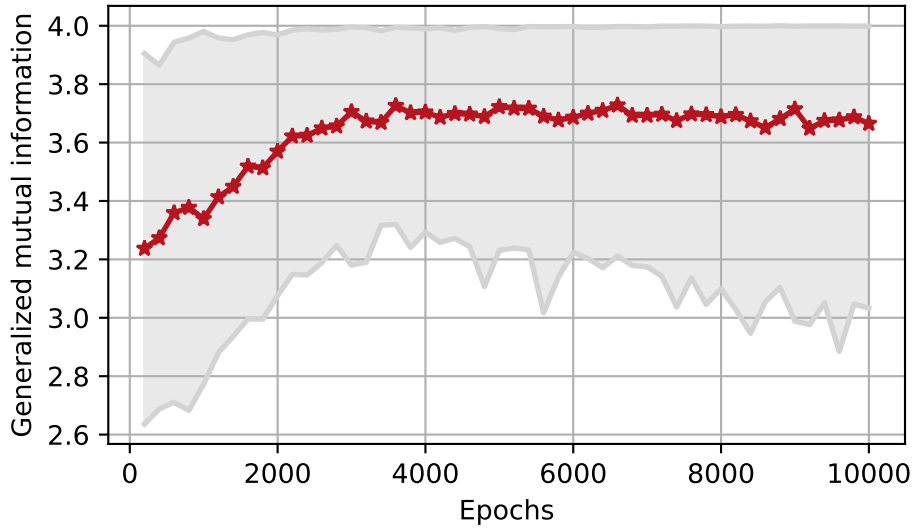


Figure 1: Monte Carlo estimation of the generalized mutual information with $\alpha = 0.5$ (from 200 samples) for π_{λ_e} where λ_e is the parameter of the neural network at epoch e . The red curve is the mean value and the gray zone is the 95% confidence interval. The learning rate used in the optimization is 0.0025.

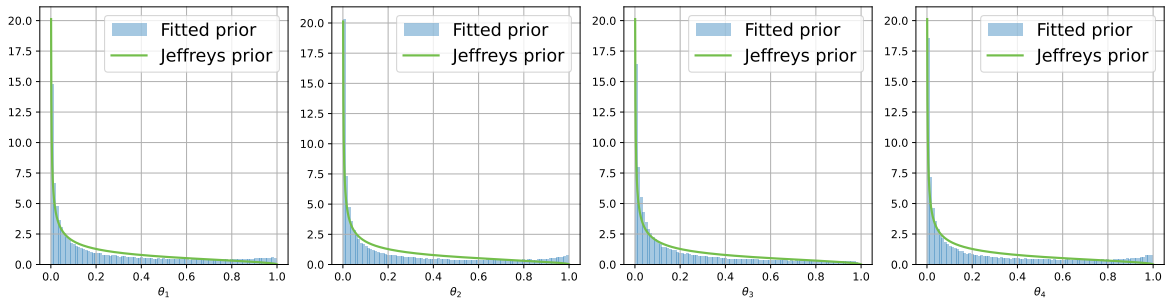


Figure 2: Histograms of the fitted prior and the marginal density functions of the Jeffreys prior $\text{Dir}(\frac{1}{2}, \frac{1}{2}, \frac{1}{2}, \frac{1}{2})$ for each dimension of θ , each histogram is obtained from 10^5 samples.

447 For the posterior distribution, we sample 10 times from the Multinomial distribution using $\theta_{true} =$
 448 $(\frac{1}{4}, \frac{1}{4}, \frac{1}{4}, \frac{1}{4})$. The covariance matrix in the proposition distribution of the Metropolis-Hastings algo-
 449 rithm is not diagonal, since we have a relation between the different components of θ , we introduce
 450 non-zero covariances. We also verified that the auto-correlation between the successive remaining
 451 samples of the Markov chain decreases rapidly on each component.

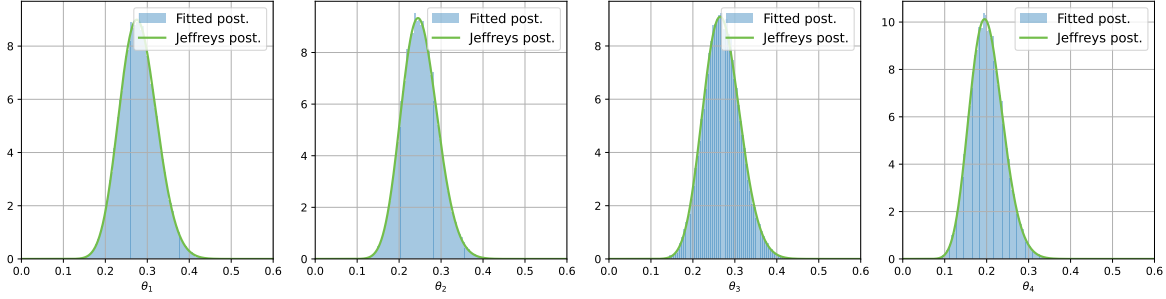


Figure 3: Histograms of the fitted posterior and the marginal density functions of the Jeffreys posterior for each dimension of θ , each histogram is obtained from $5 \cdot 10^4$ samples.

452 We notice (Figure 1) that the mutual information lies between 0 and $1/\alpha(1-\alpha) = 4$, which is coherent
 453 with the theory, the confidence interval is rather large, but the mean value has an increasing trend.
 454 In order to obtain more reliable values for the mutual information, one can use more samples in the
 455 Monte Carlo estimates at the cost of heavier computations.

456 Although the shape of the fitted prior resembles the one of the Jeffreys prior, one can notice that it
 457 tends to put more weight towards the extremities of the interval (Figure 2). The posterior distribution
 458 however is quite similar to the target Jeffreys posterior on every component (Figure 3).

459 Since the multinomial model is simple and computationally practical, we would like to quantify the
 460 effect on the output of the algorithm of some hyperparameters, namely, the divergence parameter
 461 α , the dimension of the latent space p and the addition of a hidden layer in the neural network. In
 462 order to do so, we utilize the maximum mean discrepancy (MMD) defined as:

$$\text{MMD}(\mathbb{P}, \mathbb{Q}) = \|\mu_{\mathbb{P}} - \mu_{\mathbb{Q}}\|_{\mathcal{H}},$$

463 where $\mu_{\mathbb{P}}$ and $\mu_{\mathbb{Q}}$ are respectively the kernel mean embeddings of distributions \mathbb{P} and \mathbb{Q} in a repro-
 464ducible kernel Hilbert space (RKHS) $(\mathcal{H}, \|\cdot\|_{\mathcal{H}})$, meaning: $\mu_{\mathbb{P}}(\theta') = \mathbb{E}_{\theta \sim \mathbb{P}}[K(\theta, \theta')]$ for all $\theta' \in \Theta$ and
 465 K being the kernel. The MMD is used for instance in the context of two-sample tests (Gretton et al.
 466 (2012)), whose purpose is to compare distributions. We use in our computations the Gaussian or RBF
 467 kernel:

$$K(\theta, \theta') = \exp(-0.5 \cdot \|\theta - \theta'\|_2^2),$$

468 for which the MMD is a metric, this means that the following implication:

$$\text{MMD}(\mathbb{P}, \mathbb{Q}) = 0 \implies \mathbb{P} = \mathbb{Q}$$

469 is verified with the other axioms. In practice, we consider an unbiased estimator of the MMD² given
 470 by:

$$\widehat{\text{MMD}}^2(\mathbb{P}, \mathbb{Q}) = \frac{1}{m(m-1)} \sum_{i \neq j} K(x_i, x_j) + \frac{1}{n(n-1)} \sum_{i \neq j} K(y_i, y_j) - \frac{2}{mn} \sum_{i,j} K(x_i, y_j),$$

471 where (x_1, \dots, x_m) and (y_1, \dots, y_n) are samples from \mathbb{P} and \mathbb{Q} respectively. In our case, \mathbb{P} is the distribution
 472 obtained through variational inference and \mathbb{Q} is the target Jeffreys distribution. Since the MMD can
 473 be time-consuming or memory inefficient to compute in practice for very large samples, we consider
 474 only the last $2 \cdot 10^4$ entries of our priors and posterior samples.

α	Prior	Posterior
0.10	7.07×10^{-2}	2.09×10^{-3}
0.25	7.42×10^{-2}	3.39×10^{-3}
0.50	5.26×10^{-2}	1.96×10^{-3}
0.75	7.80×10^{-2}	1.50×10^{-3}
0.90	6.15×10^{-2}	4.84×10^{-4}

Table 1: MMD values for different α -divergences at prior and posterior levels. As a reference on the prior level, when computing the criterion between two independent Dirichlet $\text{Dir}(\frac{1}{2}, \frac{1}{2}, \frac{1}{2}, \frac{1}{2})$ distributions (i.e. the Jeffreys prior) on $2 \cdot 10^4$ samples, we obtain an order of magnitude of 10^{-3} . For the posterior level, for which the marginal densities do not diverge at zero, this reference has an order of magnitude of 10^{-4} .

475 Firstly, we are interested in the effect of changing the value of α in the α -divergence, while keeping
476 $p = 50$ and the same neural network architecture. According to Table 1, the difference between α
477 values in terms of the MMD criterion is essentially inconsequential. One remark is that the mutual
478 information tends to be more unstable as α gets closer to 1. The explanation is that when α tends to
479 1, we have the approximation:

$$\hat{f}_\alpha(x) \approx \frac{x-1}{\alpha(\alpha-1)} + \frac{x \log(x)}{\alpha},$$

480 which diverges for all x because of the first term. Hence, we advise the user to avoid α values that
481 are too close to 1. In the following, we use $\alpha = 0.5$ for the divergence.

482 Secondly, we look at the effect on the dimension of the latent space denoted p for the previously
483 defined neural network architecture, but also when a second layer is added:

$$\theta = \text{Softmax} \left(W_2 \cdot \text{PReLU}_\zeta(W_1 \varepsilon + b_1) + b_2 \right),$$

484 with $W_1 \in \mathbb{R}^{10 \times p}$, $W_2 \in \mathbb{R}^{4 \times 10}$ the weight matrices and $b_1 \in \mathbb{R}^{10}$, $b_2 \in \mathbb{R}^4$ the bias vectors. The added
485 hidden layer is of dimension 10, the activation function between the two layers is the parametric
486 rectified linear unit (PReLU) which is defined as:

$$\text{PReLU}_\zeta(x) = \begin{cases} x & \text{if } x \geq 0 \\ \zeta x & \text{if } x < 0, \end{cases}$$

487 with $\zeta > 0$ a learnable parameter. The activation function is applied element-wise.

p	Prior (1 layer)	Posterior (1 layer)	Prior (2 layers)	Posterior (2 layers)
25	8.16×10^{-2}	2.02×10^{-3}	2.43×10^{-1}	2.80×10^{-2}
50	5.26×10^{-2}	1.96×10^{-3}	3.23×10^{-1}	7.09×10^{-2}
75	5.35×10^{-2}	3.79×10^{-3}	2.59×10^{-1}	1.41×10^{-2}
100	3.21×10^{-2}	2.75×10^{-3}	2.41×10^{-1}	1.47×10^{-2}
200	4.02×10^{-2}	1.84×10^{-3}	2.10×10^{-1}	2.71×10^{-2}

p	Prior (1 layer)	Posterior (1 layer)	Prior (2 layers)	Posterior (2 layers)

Table 2: MMD values for different α -divergences at prior and posterior levels. As a reference on the prior level, when computing the criterion between two independent Dirichlet $\text{Dir}(\frac{1}{2}, \frac{1}{2}, \frac{1}{2}, \frac{1}{2})$ distributions (i.e. the Jeffreys prior) on $2 \cdot 10^4$ samples, we obtain an order of magnitude of 10^{-3} . For the posterior level, for which the marginal densities do not diverge at zero, this reference has an order of magnitude of 10^{-4} .

488 Several observations can be made thanks to Table 2. Firstly, looking at the table column-wise, one
 489 can notice that the value of p tends to have little influence on the MMD values, since the order of
 490 magnitude always remains the same for each column. We remark also that the MMD values for the
 491 simple neural network with one layer are always lower than those for the neural network with the
 492 additional hidden layer when reading the table row-wise. This is true for all values of p at both the
 493 prior and the posterior level. It is important to note that these experiments were conducted with fixed
 494 values of T and U , which determine the number of samples used in the Monte Carlo approximation
 495 of the objective function's gradient. We note that increasing T and U could improve the quality of
 496 VA-RP approximations for more complex networks. However, doing so exponentially increases the
 497 computational cost of the method.

498 **4.2 Probit model**

499 We present in this section the probit model used to estimate seismic fragility curves, which was
 500 introduced by Kennedy et al. (1980), it is also referred as the log-normal model in the literature. A
 501 seismic fragility curve is the probability of failure $P_f(a)$ of a mechanical structure subjected to a
 502 seism as a function of a scalar value a derived from the seismic ground motion. The properties of the
 503 Jeffreys prior for this model are highlighted by Van Biesbroeck et al. (2024).

504 The model is defined by the observation of an i.i.d. sample $\mathbf{X} = (X_1, \dots, X_N)$ where for any i , $X_i \sim$
 505 $(Z, a) \in \mathcal{X} = \{0, 1\} \times (0, \infty)$. The distribution of the r.v. (Z, a) is parameterized by $\theta = (\theta_1, \theta_2) \in (0, \infty)^2$
 506 as:

$$\begin{cases} a \sim \text{Log-}\mathcal{N}(\mu_a, \sigma_a^2) \\ P_f(a) = \Phi\left(\frac{\log a - \log \theta_1}{\theta_2}\right) \\ Z \sim \text{Bernoulli}(P_f(a)), \end{cases}$$

507 where Φ is the cumulative distribution function of the standard Gaussian. The probit function is the
 508 inverse of Φ . The likelihood is of the form:

$$\begin{cases} L_N(\mathbf{X} | \theta) = \prod_{i=1}^N p(a_i) \prod_{i=1}^N P_f(a_i)^{Z_i} (1 - P_f(a_i))^{1-Z_i} \propto \prod_{i=1}^N P_f(a_i)^{Z_i} (1 - P_f(a_i))^{1-Z_i} \\ p(a_i) = \frac{1}{a_i \sqrt{2\pi\sigma_a^2}} \exp\left(-\frac{1}{2\sigma_a^2}(\log a_i - \mu_a)^2\right). \end{cases}$$

509 For simplicity, we denote: $\gamma_i = \frac{\log a_i - \log \theta_1}{\theta_2} = \Phi^{-1}(P_f(a_i)) = \text{probit}(P_f(a_i))$, the gradient of the
 510 log-likelihood is the following:

$$\begin{cases} \frac{\partial \log L_N(\mathbf{X} | \theta)}{\partial \theta_1} = \sum_{i=1}^N \frac{1}{\theta_1 \theta_2} \left((-Z_i) \frac{\Phi'(\gamma_i)}{\Phi(\gamma_i)} + (1 - Z_i) \frac{\Phi'(\gamma_i)}{1 - \Phi(\gamma_i)} \right) \\ \frac{\partial \log L_N(\mathbf{X} | \theta)}{\partial \theta_2} = \sum_{i=1}^N \frac{\gamma_i}{\theta_2} \left((-Z_i) \frac{\Phi'(\gamma_i)}{\Phi(\gamma_i)} + (1 - Z_i) \frac{\Phi'(\gamma_i)}{1 - \Phi(\gamma_i)} \right). \end{cases}$$

511 There is no explicit formula for the MLE, so it has to be approximated using samples. This statistical
 512 model is a more difficult case than the previous one, since no explicit formula for the Jeffreys prior is
 513 available either but it has been shown by Van Biesbroeck et al. (2024) that it is improper in θ_2 and
 514 some asymptotic rates were derived. More precisely, when $\theta_1 > 0$ is fixed,

$$\begin{cases} J(\theta) \propto 1/\theta_2 & \text{as } \theta_2 \rightarrow 0 \\ J(\theta) \propto 1/\theta_2^3 & \text{as } \theta_2 \rightarrow +\infty. \end{cases}$$

515 If we fix $\theta_2 > 0$, the prior is proper for the variable θ_1 :

$$J(\theta) \propto \frac{|\log \theta_1|}{\theta_1} \exp\left(-\frac{(\log \theta_1 - \mu_a)^2}{2\theta_2 + 2\sigma_a^2}\right) \quad \text{when } |\log \theta_1| \rightarrow +\infty.$$

516 which resembles a log-normal distribution except for the $|\log \theta_1|$ factor. Since the density of the
 517 Jeffreys prior is not explicit and can not be computed directly, the Fisher information matrix is
 518 computed in Van Biesbroeck et al. (2024) using numerical integration with Simpson's rule on a
 519 specific grid and then an interpolation is applied. We use this computation as the reference to evaluate
 520 the quality of the output of our algorithm. In the mentioned article, the posterior distribution is
 521 also computed with an adaptive Metropolis-Hastings algorithm on the variable θ , we refer to this
 522 algorithm as $\text{MH}(\theta)$ since it is different from the one mentioned in Section 3.4. More details on $\text{MH}(\theta)$
 523 are given in Gauchy (2022). We take $\mu_a = 0$, $\sigma_a^2 = 1$, $N = 500$ and $U = 500$ for the computation of the
 524 prior.

525 As for the neural network, we use a one-layer network with an \exp activation for θ_1 and a Softplus
 526 activation for θ_2 . We have that:

$$\theta = \begin{pmatrix} \theta_1 \\ \theta_2 \end{pmatrix} = \begin{pmatrix} \exp(w_1^\top \varepsilon + b_1) \\ \log(1 + \exp(w_2^\top \varepsilon + b_2)) \end{pmatrix},$$

527 with $w_1, w_2 \in \mathbb{R}^p$ the weight vectors and $b_1, b_2 \in \mathbb{R}$ the biases, thus we have $\lambda = (w_1, w_2, b_1, b_2)$.
 528 Because this architecture remains simple, it is possible to elucidate the resulting marginal distributions
 529 of θ_1 and θ_2 . The first component θ_1 follows a $\text{Log-}\mathcal{N}(b_1, \|w_1\|_2^2)$ distribution and θ_2 has an explicit
 530 density function:

$$p(\theta_2) = \frac{1}{\sqrt{2\pi\|w_2\|_2^2(1 - e^{-\theta_2})}} \exp\left(-\frac{1}{2\|w_2\|_2^2} (\log(e^{\theta_2} - 1) - b_2)^2\right).$$

531 These expressions describe the parameterized set \mathcal{P}_Λ of priors considered in the optimization problem.
 532 This set is restrictive, so that the resulting VA-RP must be interpreted as the most objective —according
 533 to the mutual information criterion— prior among the ones in \mathcal{P}_Λ . Since we do not know any explicit
 534 expression of the Jeffreys prior for this prior, we cannot provide a precise comparison between the
 535 parameterized VA-RP elucidated above and the target. However, the form of the distribution of

536 θ_1 qualitatively resembles its theoretical target. In the case of θ_2 , the asymptotic decay rates of its
 537 density function can be derived:

$$\begin{cases} p(\theta_2) \underset{\theta_2 \rightarrow 0}{=} \frac{1}{\theta_2 \sqrt{2\pi} \|w_2\|_2} \exp\left(-\frac{(\log \theta_2 - b_2)^2}{2\|w_2\|_2^2}\right); \\ p(\theta_2) \underset{\theta_2 \rightarrow \infty}{=} \frac{1}{\sqrt{2\pi} \|w_2\|_2} \exp\left(-\frac{(\theta_2 - b_2)^2}{2\|w_2\|_2^2}\right). \end{cases} \quad (12)$$

538 While $\|w_2\|_2$ does not tend toward ∞ , these decay rates strongly differ from the ones of the Jeffreys
 539 prior w.r.t. θ_2 . Otherwise, the decay rates resemble to something proportional to $(\theta_2 + 1)^{-1}$ in both
 540 directions. In our numerical computations, the optimization process yielded a VA-RP with parameters
 541 w_2 and b_2 that did not diverge to extreme values.

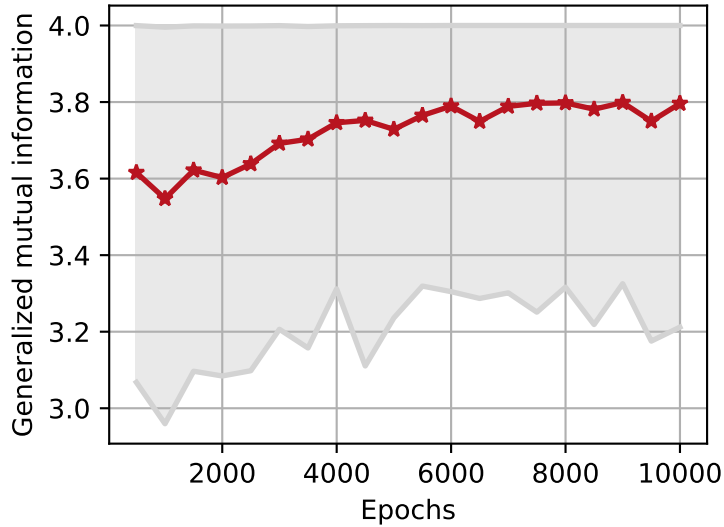


Figure 4: Monte Carlo estimation of the generalized mutual information with $\alpha = 0.5$ (from 100 samples) for π_{λ_e} where λ_e is the parameter of the neural network at epoch e . The red curve is the mean value and the gray zone is the 95% confidence interval. The learning rate used in the optimization is 0.001.

542 In Figure 4 is shown the evolution of the mutual information through the optimization of the VA-RP
 543 for the probit model. We perceive high mutual information values at the initialization, which we
 544 interpret as a result of the fact that the parametric prior on θ_1 is already quite close to its target
 545 distribution.

546 With α -divergences, using a moment constraint of the form $a(\theta_2) = \theta_2^\kappa$ for the second component
 547 is relevant here as long as $\kappa \in \left(0, \frac{2}{1+1/\alpha}\right)$, to ensure that the resulting constrained prior is indeed
 548 proper. With $\alpha = 0.5$, we take the value $\kappa = 1/8$ and we use the same neural network. The evolution
 549 of the mutual information through the optimization of the constrained VA-RP is proposed in Figure 5.
 550 In Figure 6 is presented the evolution of the constrained gap: the difference between the target and
 551 current values for the constraint.

552 For the posterior, we take as dataset 50 samples from the probit model with θ_{true} close to $(3.37, 0.43)$.
 553 For computational reasons, the Metropolis-Hastings algorithm is applied for only $5 \cdot 10^4$ iterations.
 554 An important remark is that if the size of the dataset is rather small, the probability that the data
 555 is degenerate is not negligible. By degenerate data, we refer to situations when the data points are
 556 partitioned into two disjoint subsets when classified according to a values, the posterior becomes
 557 improper because the likelihood is constant (Van Biesbroeck et al. (2024)). In such cases, the

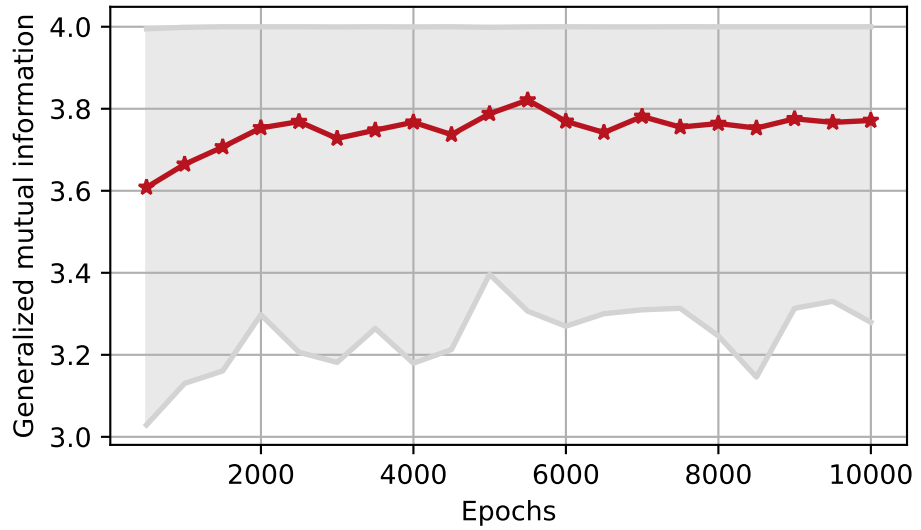


Figure 5: Monte Carlo estimation of the generalized mutual information with $\alpha = 0.5$ (from 100 samples) for π_{λ_e} where λ_e is the parameter of the neural network at epoch e . The red curve is the mean value and the gray zone is the 95% confidence interval. The learning rate used in the optimization is 0.0005.

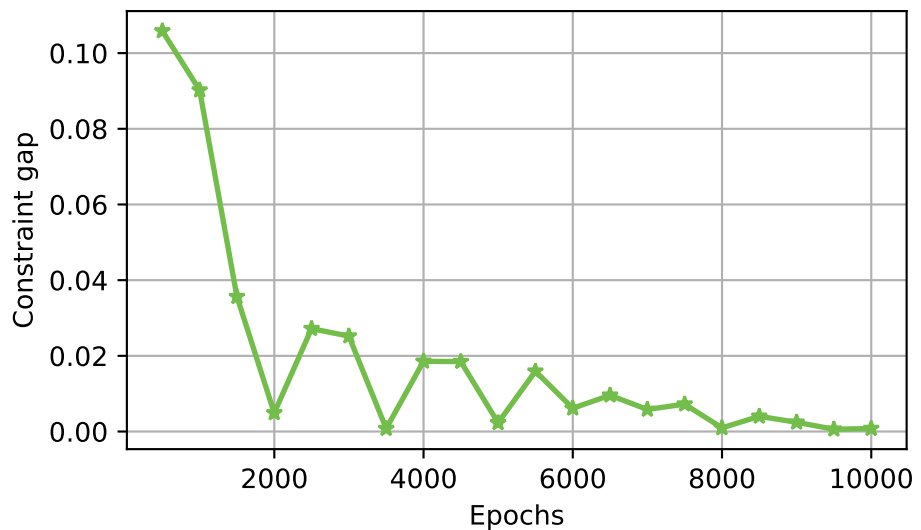


Figure 6: Evolution of the constraint value gap during training. It corresponds to the difference between the target and current values for the constraint (in absolute value)

558 convergence of the Markov chains is less apparent, the plots for this section are obtained with
559 non-degenerate datasets.

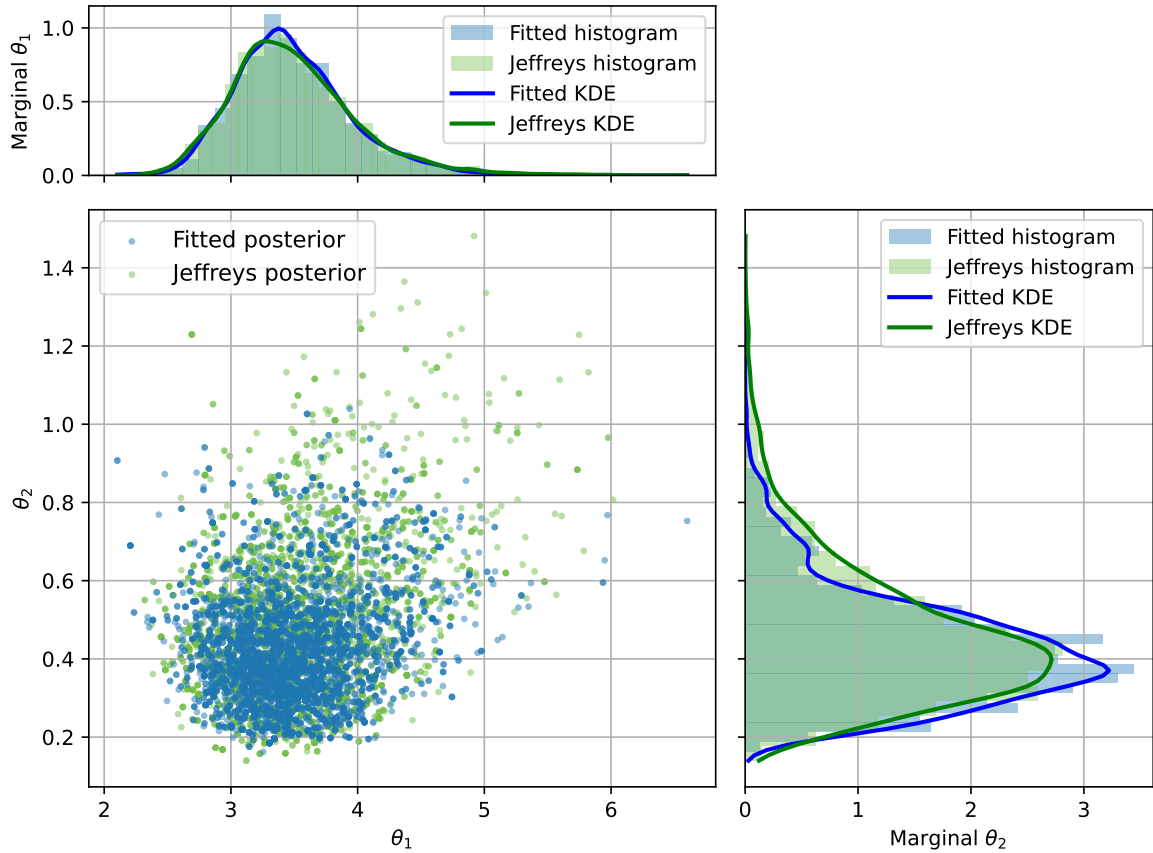


Figure 7: Scatter histogram of the unconstrained fitted posterior and the Jeffreys posterior distributions obtained from 5000 samples. Kernel density estimation is used on the marginal distributions in order to approximate their density functions with Gaussian kernels.

560 As Figure 7 shows, we obtain a relevant approximation of the true Jeffreys posterior especially on
561 the variable θ_1 , whereas a small difference is present for the tail of the distribution on θ_2 . The latter
562 remark was expected regarding the analytical study of the marginal distribution of π_λ w.r.t. θ_2 given
563 the architecture considered for the VA-RP (see Equation 12). It is interesting to see that the difference
564 between the posteriors is harder to discern in the neighborhood of $\theta_2 = 0$. Indeed, in such case where
565 the data are not degenerate, the likelihood provides a strong decay rate when $\theta_2 \rightarrow 0$ that makes the
566 influence of the prior negligible (see Van Biesbroeck et al. (2024)):

$$L_N(\mathbf{X} | \theta) \underset{\theta_2 \rightarrow 0}{\sim} \theta_2^{\|\chi\|_2^2} \exp\left(-\frac{1}{2\theta_2^2} \sum_{i=1}^N \chi_i (\log a_i - \log \theta_1)^2\right),$$

567 where $\chi \in \{0, 1\}^N$ is a non-null vector that depends on \mathbf{X} .

568 When $\theta_2 \rightarrow \infty$, however, the likelihood does not reduce the influence of the prior as it remains
569 asymptotically constant: $L_N(\mathbf{X} | \theta) \underset{\theta_2 \rightarrow \infty}{\sim} 2^{-N}$.

570 The result on the constrained case (Figure 8) is very similar to the unconstrained one.

571 Altogether, one can observe that the variational inference approach yields close results to the
572 numerical integration approach (Van Biesbroeck et al. (2024)), with or without constraints, even

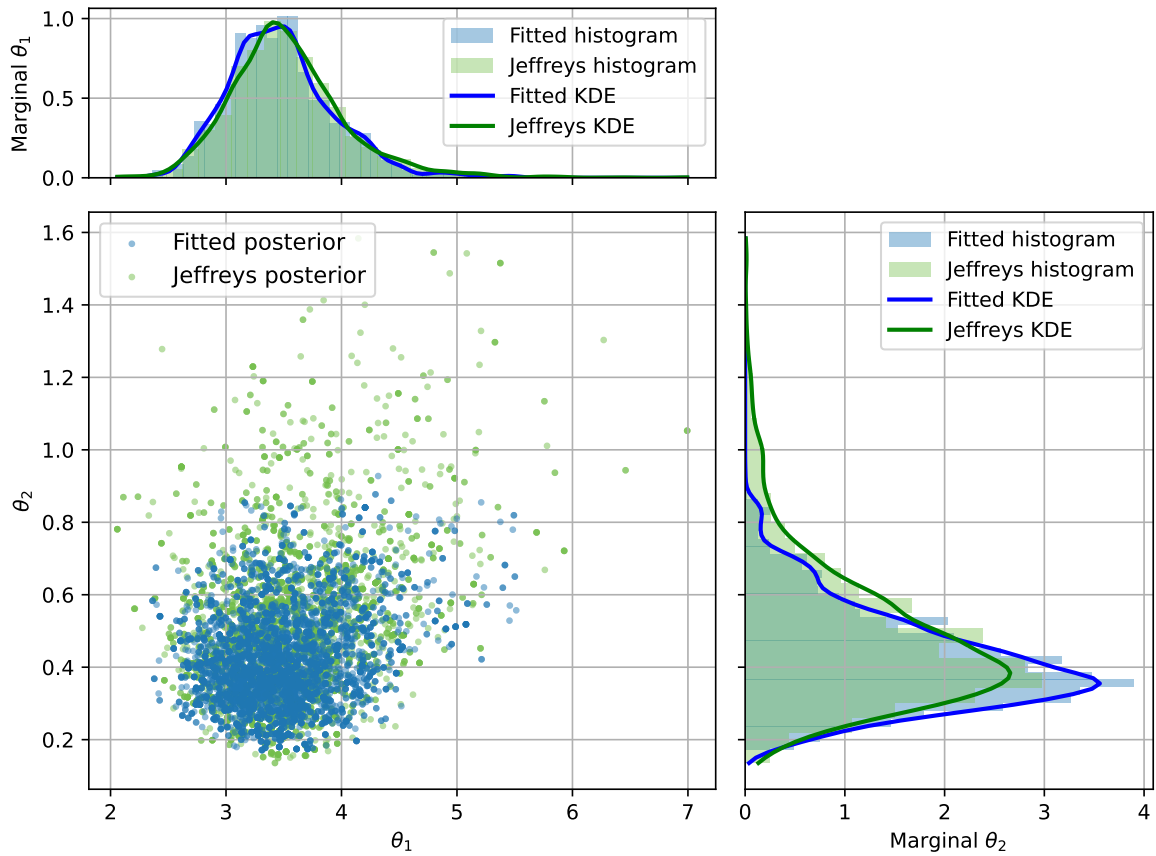


Figure 8: Scatter histogram of the constrained fitted posterior and the target posterior distributions obtained from 5000 samples. Kernel density estimation is used on the marginal distributions in order to approximate their density functions with Gaussian kernels.

573 though the matching of the decay rates w.r.t. θ_2 remains limited given the simple network that we
574 have used in this case.

575 To ascertain the relevancy of our posterior approximation, we compute the posterior mean euclidean
576 norm difference $\mathbb{E}_\theta[\|\theta - \theta_{true}\|]$ as a function of the size of the dataset. In each computation, the
577 neural network remains the same but the dataset changes by adding new entries.

578 Furthermore, in order to assess the stability of the stochastic optimization with respect to the random
579 number generator (RNG) seed, we also compute the empirical cumulative distribution functions
580 (ECDFs) for each posterior distribution. For every seed, the parameters of the neural network are
581 expected to be different, we keep the same dataset for the MCMC sampling however.

582 Finally, we compute the ECDFs for different values of the dimension of the latent space p in order to
583 quantify the sensitivity of the output distributions with respect to this hyperparameter.

584 These computations are done in the unconstrained case as well as the constrained one. The different
585 plots and details can be found in Section 6.

586 5 Conclusion

587 In this work, we developed an algorithm to perform variational approximation of objective priors
588 using a generalized definition of mutual information based on f -divergences. To enhance computa-
589 tional efficiency, we derived a lower bound of the generalized mutual information. Additionally,
590 because the objective priors of interest, which are Jeffreys priors, often yield improper posteriors, we
591 adapted the variational definition of the problem to incorporate constraints that ensure the posteriors
592 are proper.

593 Numerical experiments have been carried out on various test cases of different complexities in
594 order to validate our approach. These test cases range from purely toy models to more real-world
595 problems, namely the estimation of seismic fragility curve parameters using a probit statistical
596 model. The results demonstrate the usefulness of our approach in estimating both prior and posterior
597 distributions across various problems, including problems where the theoretical expression of the
598 target prior is cumbersome to compute.

599 Our development is supported by an open source and flexible implementation, which can be adapted
600 to a wide range of statistical models.

601 Looking forward, the approximation of the tails of the reference priors should be improved, but
602 this is a complex and general problem in the field of variational approximation. Furthermore, the
603 stability of the algorithm which seems to depend on the statistical model and the architecture of the
604 neural network is an other issue to be addressed. An extension of this work to the approximation of
605 Maximal Data Information (MDI) priors is also appealing, thanks to the fact that MDI are proper
606 under certain assumptions precised in Bousquet (2008).

607 Acknowledgement

608 This research was supported by the CEA (French Alternative Energies and Atomic Energy Commis-
609 sion) and the SEISM Institute (<https://www.institut-seism.fr/en/>).

6 Appendix

6.1 Gradient computation of the generalized mutual information

We recall that $F(x) = f(x) - xf'(x)$ and p_λ is a shortcut notation for $p_{\pi_\lambda, N}$ being the marginal distribution under π_λ . The generalized mutual information writes:

$$\begin{aligned} I_{D_f}(\pi_\lambda; L_N) &= \int_{\Theta} D_f(p_\lambda \| L_N(\cdot | \theta)) \pi_\lambda(\theta) d\theta \\ &= \int_{\Theta} \int_{\mathcal{X}^N} \pi_\lambda(\theta) L_N(\mathbf{X} | \theta) f\left(\frac{p_\lambda(\mathbf{X})}{L_N(\mathbf{X} | \theta)}\right) d\mathbf{X} d\theta. \end{aligned}$$

For each l , taking the derivative with respect to λ_l yields:

$$\begin{aligned} \frac{\partial I_{D_f}}{\partial \lambda_l}(\pi_\lambda; L_N) &= \int_{\Theta} \int_{\mathcal{X}^N} \frac{\partial \pi_\lambda}{\partial \lambda_l}(\theta) L_N(\mathbf{X} | \theta) f\left(\frac{p_\lambda(\mathbf{X})}{L_N(\mathbf{X} | \theta)}\right) d\mathbf{X} d\theta \\ &\quad + \int_{\Theta} \int_{\mathcal{X}^N} \pi_\lambda(\theta) L_N(\mathbf{X} | \theta) \frac{\partial p_\lambda}{\partial \lambda_l} \frac{1}{L_N(\mathbf{X} | \theta)}(\mathbf{X}) f'\left(\frac{p_\lambda(\mathbf{X})}{L_N(\mathbf{X} | \theta)}\right) d\mathbf{X} d\theta, \end{aligned}$$

or in terms of expectations:

$$\frac{\partial I_{D_f}}{\partial \lambda_l}(\pi_\lambda; L_N) = \frac{\partial}{\partial \lambda_l} \mathbb{E}_{\theta \sim \pi_\lambda} [\tilde{I}(\theta)] + \mathbb{E}_{\theta \sim \pi_\lambda} \left[\mathbb{E}_{\mathbf{X} \sim L_N(\cdot | \theta)} \left[\frac{1}{L_N(\mathbf{X} | \theta)} \frac{\partial p_\lambda}{\partial \lambda_l}(\mathbf{X}) f'\left(\frac{p_\lambda(\mathbf{X})}{L_N(\mathbf{X} | \theta)}\right) \right] \right],$$

where:

$$\tilde{I}(\theta) = \int_{\mathcal{X}^N} L_N(\mathbf{X} | \theta) f\left(\frac{p_\lambda(\mathbf{X})}{L_N(\mathbf{X} | \theta)}\right) d\mathbf{X}.$$

We note that the derivative with respect to λ_l does not apply to \tilde{I} in the previous equation. Using the chain rule yields:

$$\frac{\partial}{\partial \lambda_l} \mathbb{E}_{\theta \sim \pi_\lambda} [\tilde{I}(\theta)] = \frac{\partial}{\partial \lambda_l} \mathbb{E}_\varepsilon [\tilde{I}(g(\lambda, \varepsilon))] = \mathbb{E}_\varepsilon \left[\sum_{j=1}^q \frac{\partial \tilde{I}}{\partial \theta_j}(g(\lambda, \varepsilon)) \frac{\partial g_j}{\partial \lambda_l}(\lambda, \varepsilon) \right].$$

We have the following for every $j \in \{1, \dots, q\}$:

$$\begin{aligned} \frac{\partial \tilde{I}}{\partial \theta_j}(\theta) &= \int_{\mathcal{X}^N} \frac{-p_\lambda(\mathbf{X})}{L_N(\mathbf{X} | \theta)} \frac{\partial L_N}{\partial \theta_j}(\mathbf{X} | \theta) f'\left(\frac{p_\lambda(\mathbf{X})}{L_N(\mathbf{X} | \theta)}\right) + f\left(\frac{p_\lambda(\mathbf{X})}{L_N(\mathbf{X} | \theta)}\right) \frac{\partial L_N}{\partial \theta_j}(\mathbf{X} | \theta) d\mathbf{X} \\ &= \int_{\mathcal{X}^N} F\left(\frac{p_\lambda(\mathbf{X})}{L_N(\mathbf{X} | \theta)}\right) \frac{\partial L_N}{\partial \theta_j}(\mathbf{X} | \theta) d\mathbf{X} \\ &= \mathbb{E}_{\mathbf{X} \sim L_N(\cdot | \theta)} \left[\frac{\partial \log L_N}{\partial \theta_j}(\mathbf{X} | \theta) F\left(\frac{p_\lambda(\mathbf{X})}{L_N(\mathbf{X} | \theta)}\right) \right]. \end{aligned}$$

Putting everything together, we finally obtain the desired formula. The gradient of the generalized lower bound function is obtained in a very similar manner.

In what follows, we prove that the gradient of I_{D_f} as formulated in Equation 10 aligns with the form of Equation 9. We write, for $l \in \{1, \dots, L\}$:

$$\frac{\partial I_{D_f}}{\partial \lambda_l}(\pi_\lambda; L_N) = \mathbb{E}_\varepsilon \left[\sum_{j=1}^q \frac{\partial \tilde{I}}{\partial \theta_j}(g(\lambda, \varepsilon)) \frac{\partial g_j}{\partial \lambda_l}(\lambda, \varepsilon) \right] + \mathcal{G}_l,$$

624 where

$$\mathcal{G}_l = \mathbb{E}_{\theta \sim \pi_\lambda} \mathbb{E}_{\mathbf{X} \sim L_N(\cdot|\theta)} \left[\frac{1}{L_N(\mathbf{X}|\theta)} \frac{\partial p_\lambda}{\partial \lambda_l}(\mathbf{X}) f' \left(\frac{p_\lambda(\mathbf{X})}{L_N(\mathbf{X}|\theta)} \right) \right].$$

625 We remark that

$$\frac{\partial p_\lambda}{\partial \lambda_l}(\mathbf{X}) = \mathbb{E}_{\varepsilon_2} \sum_{j=1}^q \frac{\partial L_N}{\partial \theta_j}(\mathbf{X}|g(\lambda, \varepsilon_2)) \frac{\partial g_j}{\partial \lambda_l}(\lambda, \varepsilon_2).$$

626 Thus, we can develop \mathcal{G}_l as:

$$\begin{aligned} \mathcal{G}_l &= \mathbb{E}_{\varepsilon_1} \mathbb{E}_{\mathbf{X} \sim L_N(\cdot|g(\lambda, \varepsilon_1))} \mathbb{E}_{\varepsilon_2} \sum_j \frac{1}{L_N(\mathbf{X}|g(\lambda, \varepsilon_1))} f' \left(\frac{p_\lambda(\mathbf{X})}{L_N(\mathbf{X}|g(\lambda, \varepsilon_1))} \right) \frac{\partial L_N}{\partial \theta_j}(\mathbf{X}|g(\lambda, \varepsilon_2)) \frac{\partial g_j}{\partial \lambda_l}(\lambda, \varepsilon_2) \\ &= \mathbb{E}_{\varepsilon_2} \mathbb{E}_{\varepsilon_1} \mathbb{E}_{\mathbf{X} \sim L_N(\cdot|g(\lambda, \varepsilon_1))} \sum_j \frac{1}{L_N(\mathbf{X}|g(\lambda, \varepsilon_1))} f' \left(\frac{p_\lambda(\mathbf{X})}{L_N(\mathbf{X}|g(\lambda, \varepsilon_1))} \right) \frac{\partial L_N}{\partial \theta_j}(\mathbf{X}|g(\lambda, \varepsilon_2)) \frac{\partial g_j}{\partial \lambda_l}(\lambda, \varepsilon_2) \\ &= \mathbb{E}_{\varepsilon_2} \sum_{j=1}^q \frac{\partial g_j}{\partial \lambda_l}(\lambda, \varepsilon_2) \mathbb{E}_{\varepsilon_1} \mathbb{E}_{\mathbf{X} \sim L_N(\cdot|g(\lambda, \varepsilon_1))} \frac{1}{L_N(\mathbf{X}|g(\lambda, \varepsilon_1))} f' \left(\frac{p_\lambda(\mathbf{X})}{L_N(\mathbf{X}|g(\lambda, \varepsilon_1))} \right) \frac{\partial L_N}{\partial \theta_j}(\mathbf{X}|g(\lambda, \varepsilon_2)). \end{aligned}$$

627 Now, calling \tilde{K} the function defined as follows:

$$\tilde{K} : \theta \mapsto \tilde{K}(\theta) = \mathbb{E}_{\varepsilon_1} \mathbb{E}_{\mathbf{X} \sim L_N(\cdot|g(\lambda, \varepsilon_1))} \left[\frac{1}{L_N(\mathbf{X}|g(\lambda, \varepsilon_1))} f' \left(\frac{p_\lambda(\mathbf{X})}{L_N(\mathbf{X}|g(\lambda, \varepsilon_1))} \right) L_N(\mathbf{X}|\theta) \right],$$

628 we obtain that

$$\mathcal{G}_l = \mathbb{E}_{\varepsilon_2} \sum_{j=1}^q \frac{\partial g_j}{\partial \lambda_l}(\lambda, \varepsilon_2) \frac{\partial \tilde{K}}{\partial \theta_j}(g(\lambda, \varepsilon_2)).$$

629 Eventually, denoting $\tilde{\mathbf{I}} = \tilde{K} + \tilde{I}$, we have:

$$\frac{\partial I_{D_f}}{\partial \lambda_l}(\pi_\lambda; L_N) = \mathbb{E}_{\varepsilon} \left[\sum_{j=1}^q \frac{\partial \tilde{\mathbf{I}}}{\partial \theta_j}(g(\lambda, \varepsilon)) \frac{\partial g_j}{\partial \lambda_l}(\lambda, \varepsilon) \right],$$

630 which is compatible with the form of Equation 9.

6.2 Gaussian distribution with variance parameter

632 We consider a normal distribution where θ is the variance parameter: $X_i \sim \mathcal{N}(\mu, \theta)$ with $\mu \in \mathbb{R}$,
633 $\mathbf{X} \in \mathcal{X}^N = \mathbb{R}^N$ and $\theta \in \mathbb{R}_+^*$. We take $\mu = 0$. The likelihood and score functions are:

$$L_N(\mathbf{X}|\theta) = \prod_{i=1}^N \frac{1}{\sqrt{2\pi\theta}} \exp \left(-\frac{1}{2\theta}(X_i - \mu)^2 \right)$$

$$\frac{\partial \log L_N}{\partial \theta}(\mathbf{X}|\theta) = -\frac{N}{2\theta} + \frac{1}{2\theta^2} \sum_{i=1}^N (X_i - \mu)^2.$$

634 The MLE is available: $\hat{\theta}_{MLE} = \frac{1}{N} \sum_{i=1}^N X_i$. However, the Jeffreys prior is an improper distribution in
635 this case: $J(\theta) \propto 1/\theta$. Nevertheless, the Jeffreys posterior is a proper inverse-gamma distribution:

$$J_{post}(\theta|\mathbf{X}) = \Gamma^{-1} \left(\theta; \frac{N}{2}, \frac{1}{2} \sum_{i=1}^N (X_i - \mu)^2 \right).$$

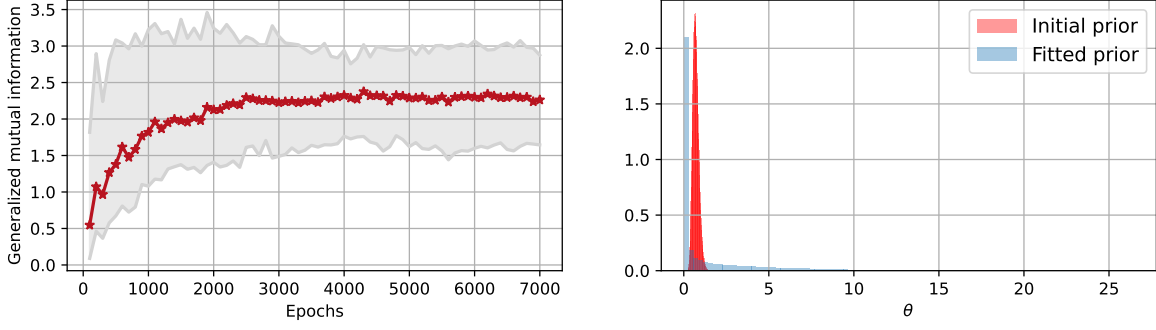


Figure 9: Left: Monte Carlo estimation of the generalized mutual information with $\alpha = 0.5$ (from 200 samples) for π_{λ_e} where λ_e is the parameter of the neural network at epoch e . The red curve is the mean value and the gray zone is the 95% confidence interval. Right: Histograms of the initial prior (at epoch 0) and the fitted prior (after training), each one is obtained from 10^5 samples. The learning rate used in the optimization is 0.025.

636 We use a neural network with one layer and a Softplus activation function. The dimension of the
 637 latent variable ε is $p = 10$.

638 We retrieve close results to those of Gauchy et al. (2023), even though we used the α -divergence
 639 instead of the classic KL-divergence (Figure 9). The evolution of the mutual information seems to be
 640 more stable during training. We can not however directly compare our result to the target Jeffrey
 641 prior since the latter is improper.

642 For the posterior distribution, we sample 10 times from the normal distribution using $\theta_{true} = 1$.

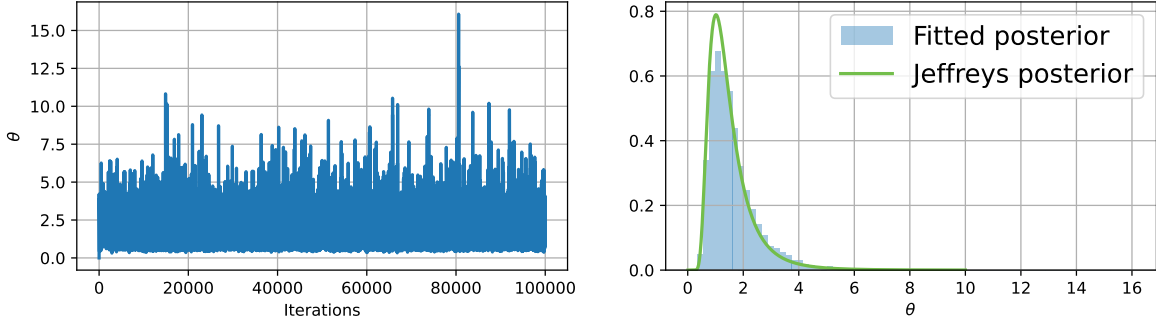


Figure 10: Left: Markov chain during the Metropolis-Hastings iterations. Right: Histogram of the fitted posterior obtained from $5 \cdot 10^4$ samples and the density function of the Jeffreys posterior.

643 As Figure 10 shows, we obtain a parametric posterior distribution which closely resembles the target
 644 distribution, even though the theoretical prior is improper.

645 In order to evaluate the performance of the algorithm for the prior, we have to add a constraint. The
 646 simplest kind of constraints are moment constraints with: $a(\theta) = \theta^\beta$, however, we can not use such a
 647 constraint here since the integrals for \mathcal{K} and c from Section 2 would diverge either at 0 or at $+\infty$.

648 If we define: $a(\theta) = \frac{1}{\theta^\beta + \theta^\tau}$ with $\beta < 0 < \tau$, then the integrals for \mathcal{K} and c are finite, because:

$$\forall \delta \geq 1, \quad \int_0^{+\infty} \frac{1}{\theta} \cdot \left(\frac{1}{\theta^\beta + \theta^\tau} \right)^\delta d\theta \leq \frac{1}{\delta} \left(\frac{1}{\tau} - \frac{1}{\beta} \right).$$

649 This function of constraint a is preferable because it yields different asymptotic rates at 0 and $+\infty$:

$$\begin{cases} a(\theta) \sim \theta^{-\beta} & \text{as } \theta \rightarrow 0 \\ a(\theta) \sim \theta^{-\tau} & \text{as } \theta \rightarrow +\infty. \end{cases}$$

650 In order to apply the algorithm, we are interested in finding:

$$\mathcal{K} = \int_0^{+\infty} \frac{1}{\theta} \cdot a(\theta)^{1/\alpha} d\theta \quad \text{and} \quad c = \int_0^{+\infty} \frac{1}{\theta} \cdot a(\theta)^{1+(1/\alpha)} d\theta.$$

651 For instance, let $\alpha = 1/2$. If $\beta = -1$, $\tau = 1$, then $\mathcal{K} = 1/2$ and $c = \pi/16$. The constraint value is
 652 $c/\mathcal{K} = \pi/8$. Thus, for this example, we only have to apply the third step of the proposed method.
 653 We use in this case a one-layer neural network with \exp as the activation function, the parametric
 654 set of priors corresponds to log-normal distributions.

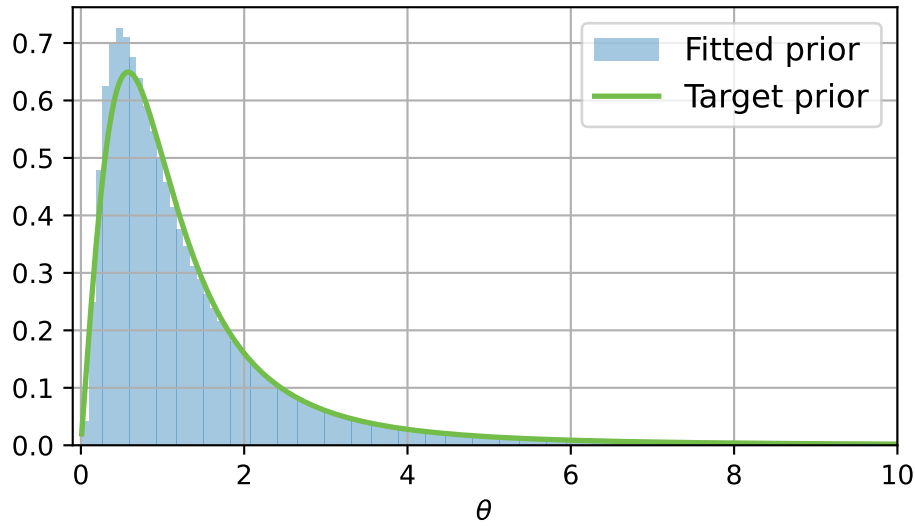


Figure 11: Histogram of the constrained fitted prior obtained from 10^5 samples, and density function of the target prior. The learning rate used in the optimization is 0.0005.

655 In this case we are able to compare prior distributions since both are proper, as Figure 11 shows, we
 656 recover a relevant result using our algorithm even with added constraints.

657 The density function of the posterior is known up to a multiplicative constant, more precisely, it
 658 corresponds to the product of the constraint function and the density function of an inverse-gamma
 659 distribution. Hence, the constant can be estimated using Monte Carlo samples from the inverse-
 660 gamma distribution in question. We apply the same approach as before in order to obtain the
 661 posterior from the parametric prior.

662 As shown in Figure 12, the parametric posterior has a shape similar to the theoretical distribution.

663 6.3 Probit model and robustness

664 As mentioned in Section 4.2 regarding the probit model, we present several additional results.

665 Figure 13 and Figure 14 show the evolution of the posterior mean norm difference as the size N of the
 666 dataset considered for the posterior distribution increases. For each value of N , 10 different datasets
 667 are used in order to quantify the variability of said error. The proportion of degenerate datasets is

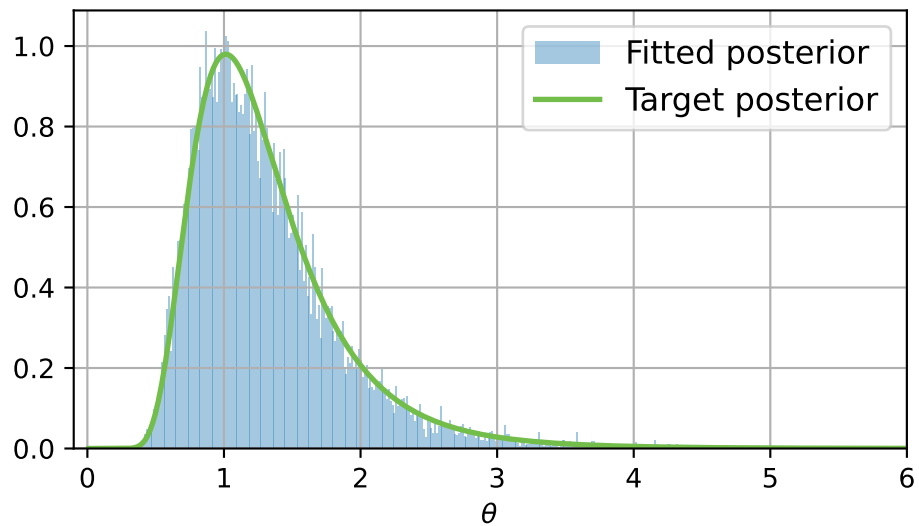


Figure 12: Histogram of the fitted posterior obtained from $5 \cdot 10^4$ samples, and density function of the target posterior.

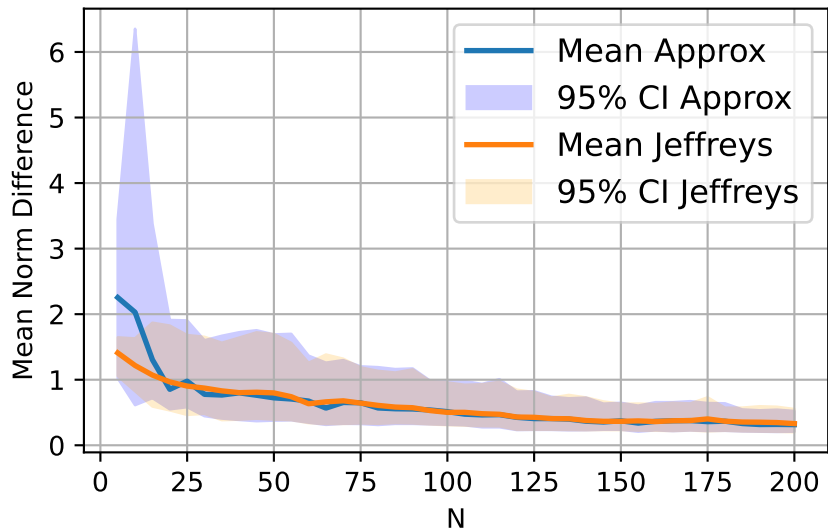


Figure 13: Mean norm difference as a function of the size N of the dataset for the unconstrained fitted posterior and the Jeffreys posterior. For each value of N , 10 different datasets are considered from which we obtain 95% confidence intervals.

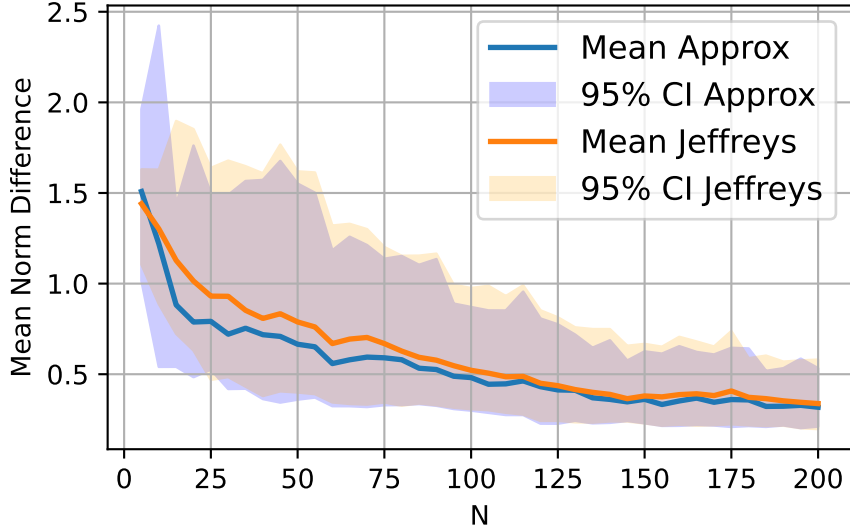


Figure 14: Mean norm difference as a function of the size N of the dataset for the constrained fitted posterior and the Jeffreys posterior. For each value of N , 10 different datasets are considered from which we obtain 95% confidence intervals.

668 rather high when $N = 5$ or $N = 10$, the consequence is that the approximation tends to be more
 669 unstable. The main observation is that the error is decreasing in all cases when N increases, also, the
 670 behaviour of the error for the fitted distributions on one hand, and the behaviour for the Jeffreys
 671 distribution on the other hand are quite similar in terms of mean value and confidence intervals.

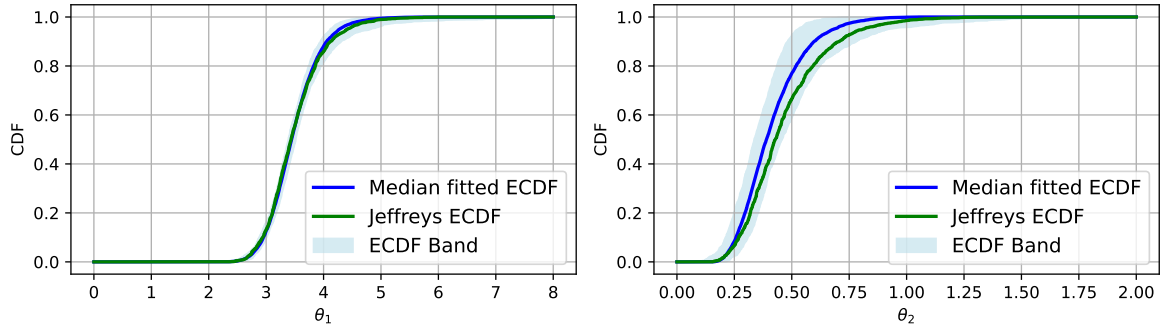


Figure 15: Empirical cumulative distribution functions for the unconstrained fitted posterior and the Jeffreys posterior using 5000 samples. The band is obtained by computing the ECDFs over 100 different seeds and monitoring the maximum and minimum ECDF values for each θ .

672 Figure 15 and Figure 16 compare the empirical cumulative distribution functions of the fitted posterior
 673 and the Jeffreys posterior. In the unconstrained case, one can observe that the ECDFs are very close
 674 for θ_1 , whereas the variability is slightly higher for θ_2 although still reasonable. When imposing
 675 a constraint on θ_2 , one remarks that the variability of the result is higher. The Jeffreys ECDF is
 676 contained in the band when θ_2 is close to zero, but not when θ_2 increases ($\theta_2 > 0.5$). This is coherent
 677 with the previous scatter histograms where the Jeffreys posterior on θ_2 tends to have a heavier tail
 678 than the variational approximation.

679 Altogether, despite the stochastic nature of the developed algorithm, we consider that the result
 680 tends to be reasonably robust to the RNG seed for the optimization part, and robust to the dataset
 681 used for the posterior distribution for the MCMC part.

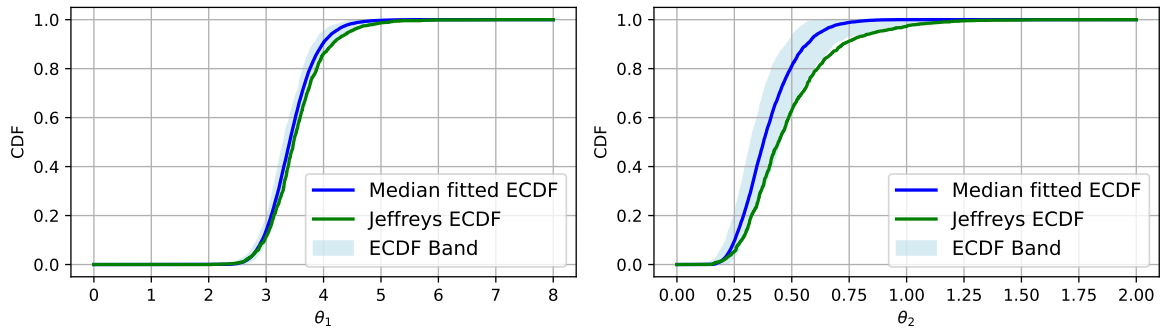


Figure 16: Empirical cumulative distribution functions for the constrained fitted posterior and the Jeffreys posterior using 5000 samples. The band is obtained by computing the ECDFs over 100 different seeds and monitoring the maximum and minimum ECDF values for each θ .

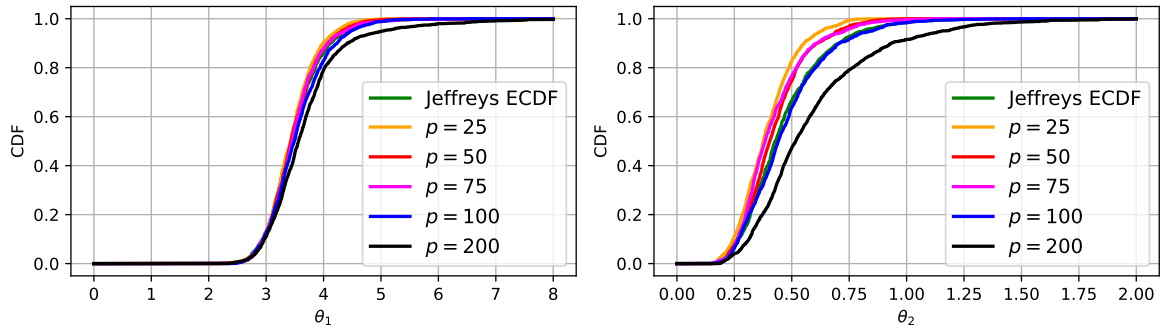


Figure 17: Empirical cumulative distribution functions for the constrained fitted posterior and the Jeffreys posterior using 5000 samples. The band is obtained by computing the ECDFs over 100 different seeds and monitoring the maximum and minimum ECDF values for each θ .

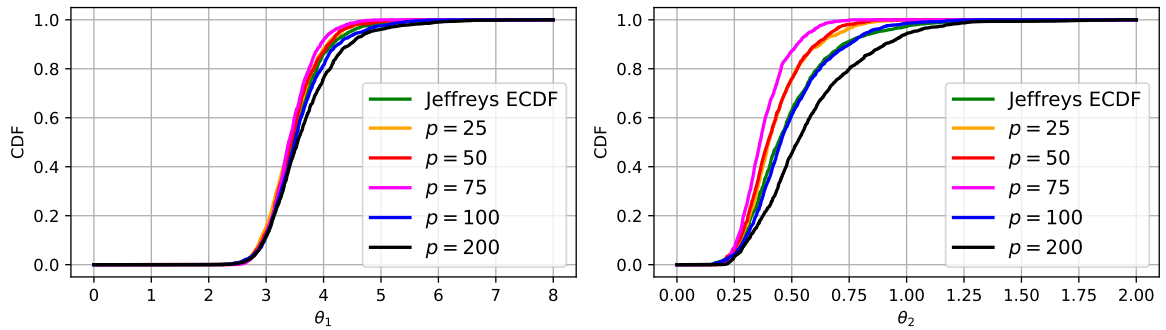


Figure 18: Empirical cumulative distribution functions for the constrained fitted posterior and the Jeffreys posterior using 5000 samples. The band is obtained by computing the ECDFs over 100 different seeds and monitoring the maximum and minimum ECDF values for each θ .

682 Figure 17 and Figure 18 compare the empirical cumulative distribution functions of the fitted posterior
683 and the Jeffreys posterior when several values for the latent space dimension p are considered. We
684 observe that in both the unconstrained case and the constrained case, the ECDFs are quite different
685 for the θ_1 component when p varies, these differences are even more notable on θ_2 . We remark that
686 the fitted distributions for $p = 100$ are the closest to the target Jeffreys distributions compared to
687 lower values of p , but this is likely due to random chance, since when we keep increasing p to 200,
688 we obtain a worse approximation of the Jeffreys distributions. This last case is expected to be less
689 stable due to the higher number of parameters to be fitted. The output of the algorithm is quite
690 sensitive with respect to the choice of p for the probit model, whereas for the multinomial model we
691 noticed that this choice had little effect on the MMD values.

692 A possible explanation for this behavior can be obtained by looking at the approximation of the
693 target prior given in reference Van Biesbroeck et al. (2025), which exhibits a correlation between θ_1
694 and θ_2 . Thus, this allows us to numerically verify that even in the case where the prior is proper,
695 the conditional variance of θ_2 and the variance of θ_1 are infinite due to the heavy tail in $\theta_2 \rightarrow \infty$.
696 The instability of the algorithm therefore seems to be due to the fact that it aims to approach a
697 distribution of infinite variance.

698 References

699 Basir, Shamsulhaq, and Inanc Senocak. 2023. “An Adaptive Augmented Lagrangian Method for
700 Training Physics and Equality Constrained Artificial Neural Networks.” <https://arxiv.org/abs/2306.04904>.

702 Berger, James O., Jose M. Bernardo, and Dongchu Sun. 2015. “Overall Objective Priors.” *Bayesian
703 Analysis* 10 (1). <https://doi.org/10.1214/14-ba915>.

704 Berger, James O., and José M Bernardo. 1992a. “Ordered Group Reference Priors with Application to
705 the Multinomial Problem.” *Biometrika* 79 (1): 25–37. <https://doi.org/10.1093/biomet/79.1.25>.

706 Berger, James O., and José M. Bernardo. 1992b. “On the Development of Reference Priors.” *Bayesian
707 Statistics* 4 (November).

708 Berger, James O., José M. Bernardo, and Dongchu Sun. 2009. “The formal definition of reference
709 priors.” *The Annals of Statistics* 37 (2): 905–38. <https://doi.org/10.1214/07-AOS587>.

710 Bernardo, José M. 1979a. “Expected Information as Expected Utility.” *The Annals of Statistics* 7 (3):
711 686–90. <https://doi.org/10.1214/aos/1176344689>.

712 ———. 1979b. “Reference Posterior Distributions for Bayesian Inference.” *Journal of the Royal
713 Statistical Society. Series B* 41 (2): 113–47. <https://doi.org/10.1111/j.2517-6161.1979.tb01066.x>.

714 ———. 2005. “Reference Analysis.” In *Bayesian Thinking*, edited by D. K. Dey and C. R. Rao, 25:17–90.
715 Handbook of Statistics. Elsevier. [https://doi.org/10.1016/S0169-7161\(05\)25002-2](https://doi.org/10.1016/S0169-7161(05)25002-2).

716 Bioche, Christèle, and Pierre Druilhet. 2016. “Approximation of Improper Priors.” *Bernoulli* 22 (3):
717 1709–28. <https://doi.org/10.3150/15-bej708>.

718 Bousquet, Nicolas. 2008. “Eliciting Vague but Proper Maximal Entropy Priors in Bayesian Experiments.” *Statistical Papers* 51 (3): 613–28. <https://doi.org/10.1007/s00362-008-0149-9>.

720 Clarke, Bertrand S., and Andrew R. Barron. 1994. “Jeffreys’ Prior Is Asymptotically Least Favorable
721 Under Entropy Risk.” *Journal of Statistical Planning and Inference* 41 (1): 37–60. [https://doi.org/10.1016/0378-3758\(94\)90153-8](https://doi.org/10.1016/0378-3758(94)90153-8).

723 D’Andrea, Vera L. D. AND Aljohani, Amanda M. E. AND Tomazella. 2021. “Objective Bayesian
724 Analysis for Multiple Repairable Systems.” *PLOS ONE* 16 (November): 1–19. <https://doi.org/10.1371/journal.pone.0258581>.

726 Gao, Yansong, Rahul Ramesh, and Pratik Chaudhari. 2022. “Deep Reference Priors: What Is the
727 Best Way to Pretrain a Model?” In *Proceedings of the 39th International Conference on Machine
728 Learning*, 162:7036–51. Proceedings of Machine Learning Research. PMLR. <https://Proceedings>.

729 mlr.press/v162/gao22d.html.

730 Gauchy, Clément. 2022. “Uncertainty quantification methodology for seismic fragility curves of
731 mechanical structures : Application to a piping system of a nuclear power plant.” Theses, Institut
732 Polytechnique de Paris. <https://theses.hal.science/tel-04102809>.

733 Gauchy, Clément, Antoine Van Biesbroeck, Cyril Feau, and Josselin Garnier. 2023. “Inférence
734 Variationnelle de Lois a Priori de Référence.” In *Proceedings Des 54èmes Journées de Statistiques*
735 (JdS). SFDS. <https://jds2023.sciencesconf.org/resource/page/id/19>.

736 Gelman, Andrew, John B. Carlin, Hal S. Stern, David B. Dunson, Aki Vehtari, and Donald B. Rubin.
737 2013. “Bayesian Data Analysis, Third Edition.” In, 293–300. Chapman; Hall/CRC. <https://doi.org/10.1201/b16018>.

738 Ghosal, Subhashis, and Tapas Samanta. 1997. “EXPANSION OF BAYES RISK FOR ENTROPY LOSS
739 AND REFERENCE PRIOR IN NONREGULAR CASES.” *Statistics & Risk Modeling* 15 (2): 129–40.
740 <https://doi.org/doi:10.1524/strm.1997.15.2.129>.

741 Gretton, Arthur, Karsten M. Borgwardt, Malte J. Rasch, Bernhard Schölkopf, and Alexander Smola.
742 2012. “A Kernel Two-Sample Test.” *Journal of Machine Learning Research* 13 (25): 723–73.
743 <http://jmlr.org/papers/v13/gretton12a.html>.

744 Gu, Mengyang, and James O. Berger. 2016. “Parallel partial Gaussian process emulation for computer
745 models with massive output.” *The Annals of Applied Statistics* 10 (3): 1317–47. <https://doi.org/10.1214/16-AOAS934>.

746 Jang, Eric, Shixiang Gu, and Ben Poole. 2017. “Categorical Reparameterization with Gumbel-Softmax.”
747 In *Proceedings of the 5th International Conference on Learning Representations (ICLR)*. Toulon,
748 France. <https://doi.org/10.48550/arXiv.1611.01144>.

749 Jaynes, E. T. 1957. “Information Theory and Statistical Mechanics.” *Phys. Rev.* 106 (May): 620–30.
750 <https://doi.org/10.1103/PhysRev.106.620>.

751 Jeffreys, Harold. 1946. “An Invariant Form for the Prior Probability in Estimation Problems.” *Proceedings
752 of the Royal Society of London. Series A. Mathematical and Physical Sciences* 186 (1007):
753 453–61. <https://doi.org/10.1098/rspa.1946.0056>.

754 Kass, Robert E., and Larry Wasserman. 1996. “The Selection of Prior Distributions by Formal Rules.”
755 *Journal of the American Statistical Association* 91 (435): 1343–70. <https://doi.org/10.1080/01621459.1996.10477003>.

756 Kennedy, Robert P., C. Allin Cornell, Robert D. Campbell, Stan J. Kaplan, and F. Harold. 1980.
757 “Probabilistic Seismic Safety Study of an Existing Nuclear Power Plant.” *Nuclear Engineering and
758 Design* 59 (2): 315–38. [https://doi.org/10.1016/0029-5493\(80\)90203-4](https://doi.org/10.1016/0029-5493(80)90203-4).

759 Kingma, Diederik P., and Jimmy Ba. 2017. “Adam: A Method for Stochastic Optimization.” In
760 *Proceedings of the 3rd International Conference on Learning Representations (ICLR)*. San Diego,
761 USA. <https://doi.org/10.48550/arXiv.1412.6980>.

762 Kingma, Diederik P., and Max Welling. 2014. “Auto-Encoding Variational Bayes.” In *Proceedings
763 of the 2nd International Conference on Learning Representations (ICLR)*. Banff, Canada. <https://doi.org/10.48550/arXiv.1312.6114>.

764 ——. 2019. “An Introduction to Variational Autoencoders.” *Foundations and Trends® in Machine
765 Learning* 12 (4): 307–392. <https://doi.org/10.1561/2200000056>.

766 Kobyzhev, Ivan, Simon J. D. Prince, and Marcus A. Brubaker. 2021. “Normalizing Flows: An Intro-
767 duction and Review of Current Methods.” *IEEE Transactions on Pattern Analysis and Machine
768 Intelligence* 43 (11): 3964–79. <https://doi.org/10.1109/TPAMI.2020.2992934>.

769 Lafferty, John D., and Larry A. Wasserman. 2001. “Iterative Markov Chain Monte Carlo Computation
770 of Reference Priors and Minimax Risk.” In *Proceedings of the 17th Conference in Uncertainty in
771 Artificial Intelligence (UAI)*, edited by Jack S. Breese and Daphne Koller, 293–300. Seattle, USA:
772 Morgan Kaufmann. <https://doi.org/10.48550/arXiv.1301.2286>.

773 Li, Hanmo, and Mengyang Gu. 2021. “Robust Estimation of SARS-CoV-2 Epidemic in US Counties.”
774 *Scientific Reports* 11 (11841): 2045–2322. <https://doi.org/10.1038/s41598-021-90195-6>.

779 Liu, Ruitao, Arijit Chakrabarti, Tapas Samanta, Jayanta K. Ghosh, and Malay Ghosh. 2014. “On
 780 Divergence Measures Leading to Jeffreys and Other Reference Priors.” *Bayesian Analysis* 9 (2):
 781 331–70. <https://doi.org/10.1214/14-BA862>.

782 MacKay, D. J. C. 2003. *Information Theory, Inference, and Learning Algorithms*. Copyright Cambridge
 783 University Press.

784 Marzouk, Y., T. Moselhy, M. Parno, and A. Spantini. 2016. “Sampling via Measure Transport: An
 785 Introduction.” In *Handbook of Uncertainty Quantification*, 1–41. Cham: Springer International
 786 Publishing. https://doi.org/10.1007/978-3-319-11259-6_23-1.

787 Muré, Joseph. 2018. “Objective Bayesian Analysis of Kriging Models with Anisotropic Correlation
 788 Kernel.” PhD thesis, Université Sorbonne Paris Cité. https://theses.hal.science/tel-02184403/file/MURE_Joseph_2_complete_20181005.pdf.

789 Nalisnick, Eric, and Padhraic Smyth. 2017. “Learning Approximately Objective Priors.” In *Proceedings
 790 of the 33rd Conference on Uncertainty in Artificial Intelligence (UAI)*. Sydney, Australia: Association
 791 for Uncertainty in Artificial Intelligence (AUAI). <https://doi.org/10.48550/arXiv.1704.01168>.

792 Natarajan, Ranjini, and Robert E. Kass. 2000. “Reference Bayesian Methods for Generalized Linear
 793 Mixed Models.” *Journal of the American Statistical Association* 95 (449): 227–37. <https://doi.org/10.1080/01621459.2000.10473916>.

794 Nocedal, Jorge, and Stephen J. Wright. 2006. “Numerical Optimization.” In *Springer Series in
 795 Operations Research and Financial Engineering*, 497–528. Springer New York. https://doi.org/10.1007/978-0-387-40065-5_17.

796 Papamakarios, George, Eric Nalisnick, Danilo Jimenez Rezende, Shakir Mohamed, and Balaji Laksh-
 797 minarayanan. 2021. “Normalizing Flows for Probabilistic Modeling and Inference.” *Journal of
 798 Machine Learning Research* 22 (57): 1–64. <http://jmlr.org/papers/v22/19-1028.html>.

799 Paszke, Adam, Sam Gross, Francisco Massa, Adam Lerer, James Bradbury, Gregory Chanan, Trevor
 800 Killeen, et al. 2019. “PyTorch: An Imperative Style, High-Performance Deep Learning Library.”
 801 In *Advances in Neural Information Processing Systems*, edited by H. Wallach, H. Larochelle, A.
 802 Beygelzimer, F. dAlché-Buc, E. Fox, and R. Garnett. Vol. 32. Curran Associates, Inc. https://proceedings.neurips.cc/paper_files/paper/2019/file/bdbca288fee7f92f2bfa9f7012727740-Paper.pdf.

803 Paulo, Rui. 2005. “Default priors for Gaussian processes.” *The Annals of Statistics* 33 (2): 556–82.
 804 <https://doi.org/10.1214/009053604000001264>.

805 Press, S James. 2009. *Subjective and Objective Bayesian Statistics: Principles, Models, and Applications*.
 806 John Wiley & Sons.

807 Reid, N, R Mukerjee, and DAS Fraser. 2003. “Some Aspects of Matching Priors.” *Lecture Notes-
 808 Monograph Series*, 31–43.

809 Simpson, Daniel, Håvard Rue, Andrea Riebler, Thiago G. Martins, and Sigrunn H. Sørbye. 2017.
 810 “Penalising Model Component Complexity: A Principled, Practical Approach to Constructing
 811 Priors.” *Statistical Science* 32 (1): 1–28. <https://doi.org/10.1214/16-STS576>.

812 Soofi, Ehsan S. 2000. “Principal Information Theoretic Approaches.” *Journal of the American Statistical
 813 Association* 95 (452): 1349–53. <https://doi.org/10.1080/01621459.2000.10474346>.

814 Van Biesbroeck, Antoine. 2024a. “Generalized Mutual Information and Their Reference Priors Under
 815 Csizar f-Divergence.” <https://arxiv.org/abs/2310.10530>.

816 ——. 2024b. “Properly Constrained Reference Priors Decay Rates for Efficient and Robust Posterior
 817 Inference.” <https://arxiv.org/abs/2409.13041>.

818 Van Biesbroeck, Antoine, Clément Gauchy, Cyril Feau, and Josselin Garnier. 2024. “Reference Prior
 819 for Bayesian Estimation of Seismic Fragility Curves.” *Probabilistic Engineering Mechanics* 76
 820 (April): 103622. <https://doi.org/10.1016/j.probengmech.2024.103622>.

821 ——. 2025. “Robust a Posteriori Estimation of Probit-Lognormal Seismic Fragility Curves via
 822 Sequential Design of Experiments and Constrained Reference Prior.” <https://arxiv.org/abs/2503.07343>.

823 Zellner, Arnold. 1996. “Models, Prior Information, and Bayesian Analysis.” *Journal of Econometrics*

Submitted